

Review

# Nanocomposite Membranes for Liquid and Gas Separations from the Perspective of Nanostructure Dimensions

Pei Sean Goh \*, Kar Chun Wong and Ahmad Fauzi Ismail

Advanced Membrane Technology Research Centre (AMTEC), School of Chemical and Energy Engineering, Faculty of Engineering, Universiti Teknologi Malaysia, Johor Bahru 81310, Malaysia; amtec@utm.my (K.C.W.); afauzi@utm.my (A.F.I.)

\* Correspondence: peisean@petroleum.utm.my; Tel.: +60-7-553-5812

Received: 26 September 2020; Accepted: 19 October 2020; Published: 21 October 2020



**Abstract:** One of the critical aspects in the design of nanocomposite membrane is the selection of a well-matched pair of nanomaterials and a polymer matrix that suits their intended application. By making use of the fascinating flexibility of nanoscale materials, the functionalities of the resultant nanocomposite membranes can be tailored. The unique features demonstrated by nanomaterials are closely related to their dimensions, hence a greater attention is deserved for this critical aspect. Recognizing the impressive research efforts devoted to fine-tuning the nanocomposite membranes for a broad range of applications including gas and liquid separation, this review intends to discuss the selection criteria of nanostructured materials from the perspective of their dimensions for the production of high-performing nanocomposite membranes. Based on their dimension classifications, an overview of the characteristics of nanomaterials used for the development of nanocomposite membranes is presented. The advantages and roles of these nanomaterials in advancing the performance of the resultant nanocomposite membranes for gas and liquid separation are reviewed. By highlighting the importance of dimensions of nanomaterials that account for their intriguing structural and physical properties, the potential of these nanomaterials in the development of nanocomposite membranes can be fully harnessed.

**Keywords:** nanocomposite membranes; inorganic nanomaterials; nanomaterials; liquid separation; gas separation

## 1. Introduction

Membrane-based separation has earned its place in a wide spectrum of commercial applications. Over the last few decades, progressive growth has been witnessed in the application of membrane technology in wastewater treatment, desalination, gas separation and energy generation [1–3]. With its commercial attractiveness based on advantages such as high energy efficiency, low carbon footprint and operational simplicity, attaining a reliable and sustainable separation process based on membrane technology is one of the greatest areas of interest in this field [4,5]. The membrane is known as the heart of the entire separation process. The separation performance and efficiencies are closely related to the intrinsic properties of membranes. A highly selective membrane material ensures high purity; a highly permeable membrane material allows sufficiently high productivity for large-scale application; a fouling resistant membrane material extends the shelf lifespan of the liquid separation membrane module which leads to cost saving. Although polymeric membranes are currently dominating the membrane market, there are intensive efforts to develop high-performance membranes with multifunctional physicochemical properties [6,7].

Nanotechnology has been dynamically adapted to a broad range of modern applications, including membrane development. The emergence of nanoscience is also concerned with the production of new or enhanced materials. Nanomaterials are the subject of intense research and are known to be highly versatile materials, in which their physical and chemical properties can be flexibly tailored [8]. At the atomic level, this can be accomplished by tuning the elemental composition, atomic/molecular arrangement and nanomaterial dimension via a bottom-up approach [9]. At a macroscopic level, post-synthesis modifications can be performed on the device or system to create new functionalities and capabilities. The interdisciplinary research of material chemistry and engineering applications hold the key to heightened material performance. Tapping these new opportunities, innovations have been constantly made to resolve the pertinent issues of membrane processes, including addressing the trade-off between selectivity and productivity as well as membrane fouling, membrane aging and plasticization [10]. One such innovation which has created new horizons in membrane-based separation processes is the development of nanocomposite membranes—an emerging generation of membrane which amalgamates polymers and inorganic materials as one entity [11]. The application of nanocomposite membranes has been extended in various separation processes and has made great strides in performance enhancement. The interplay between the two entities uniquely combine the benefits of each component and diminish their inherent limitations [12].

In the so-called nanocomposite membranes, the nanomaterials can be integrated with polymer matrix in several ways, including (i) the most common direct blending of nanomaterials with polymers to form mixed matrix membranes (MMMs) [13] and (ii) the post-incorporation of nanomaterials onto the preformed membrane surface through surface assembly, coating or grafting [14]. For thin-film composite membranes used for gas separation, nanofiltration (NF), reverse osmosis (RO) and forward osmosis (FO), the nanocomposite membranes can be prepared in more flexible manners, i.e., by incorporating the nanofillers into the substrate and/or the selective layer and by surface architecture [15]. Regardless of the structures and configurations, nanocomposite membranes have been hailed as one of the game changers in membrane technology. One of the most critical aspects in the development of nanocomposite membrane is a proper selection of both nanomaterials (dispersed phase) and polymer (continuous phase). Defining a set of questions related to material selection, such as what is the intended use and what the specific properties of the membrane are needed for that use can provide fruitful guidelines to visualize the outcome of the function-led membranes. Understanding the properties of materials is particularly crucial, not solely from a fundamental point of view, but also because knowledge in this aspect forms a strong basis for the development of nanocomposite membranes and their resultant performance. It is also of paramount interest for tailoring the membrane properties. The advent of characterization techniques provides adequate information about a newly discovered nanomaterial, hence helping to establish function-structure relationship.

Nanomaterials can be characterized by multiple parameters including the dimension, surface chemistry and crystal structures. A broad classification based on their geometry and dimension allow all nanomaterials to be classified into four groups i.e., zero-dimension (0D), one-dimensional (1D), 2-dimensional (2D) and three-dimensional (3D) [16–18]. Accordingly, 0D nanomaterials are mostly spherical or quasi-spherical, dots and clustered nanoparticles with all the dimension confined within nanoscale below 100 nm; 1D nanomaterials are commonly featured as nanotubes, nanorods and nanowires where one of their dimensions is beyond 100 nm. The typical examples of 2D nanomaterials are sheet-like graphene and hexagonal boron nitride with only one dimension falls within single or few atomic thicknesses. In 3D nanomaterial such as polycrystal and microporous framework assemblies, all dimensions of the structure are in the microscale range. In the context of nanocomposite membranes, the surface chemistry of the nanomaterials used as a nanofiller or surface modifier of membranes such as their surface charges, hydrophilicity, functional groups are critical aspects that affects the physicochemical properties of the resultant membranes [19,20]. On the other hand, the dimension of nanostructures imparts more significant influence on the nanomaterial distribution patterns, the transport behavior across the nanofiller, as well as the interactions and the accessibility of

the nanostructures to the surrounding matrix or species. Understanding of the structural properties and uniqueness is an important tool for the development of a nanocomposite membrane that serves that right purpose. While the surface chemistry aspect, particularly that related to surface functionalization or modification of nanomaterials, has been comprehensively covered in considerable review articles, the important roles of nanostructure dimension has not been given equal emphasis.

Considering the relevance of nanocomposite membrane in heightening membrane separation performances, a rich literature on the preparation and performance evaluations of nanocomposite membranes for various membrane-based liquid and gas separation processes already exists. Most reviews put more emphasize on the progressive advances in the development of nanocomposite membranes. The preparation and applications of nanomaterials with different dimensions have been comprehensively reviewed [21–23]. The potentials of 2D materials in enhancing the membrane separation performance are among the most discussed topics [24–29]. With the existing contributions, this review does not intend to provide an exhaustive review on the preparation and performance evaluation of nanocomposite membrane-containing nanomaterials of various dimensions, but it is aimed to outline the importance of selecting a nanostructure with an appropriate dimension that caters for its application. A brief overview of nanostructures commonly used for water and gas separation nanocomposite membranes is first presented based on their dimensional uniqueness. The correlations between nanostructure dimensions and the intended application of the nanocomposite is discussed based on some recent exemplary works. The synergistic effects of hybrids made from two or more dimensionally different nanostructures as well as the orientation of 1D and 2D anisotropic nanomaterials in the nanocomposite membranes are also discussed. Finally, some research directions that are essential for the further advancement of nanocomposite membranes with emphasis on the dimensional advantages are highlighted.

## 2. Dimension Plays Its Role: An Overview

Although the chemical composition remains unchanged, the structural and chemical parameters are significantly influenced by their dimensions, i.e., geometries and structures [30]. The most classical example is carbon element which shows unique allotropy- the existence of a range of distinctive molecular structures from the same element [31]. The allotropes exist in multidimensions, including 0D fullerene, 1D carbon nanotube (CNT), 2D graphene and 3D graphite. These carbon allotropes, especially the low-dimensional CNT and graphene have been extensively applied for the development of nanocomposite membrane owing to their outstanding novel features [32]. Due to the variation in their structural geometries as well as the chemical bonds and interactions within the structure, these allotropes are characterized by drastically different chemical properties. Nanostructured titanium dioxide or titania also can be synthesized in several dimensions, the 0D spherical nanoparticle, 1D titania nanotubes and 2D titania nanofilm as well as the more complex hierarchical 3D titania with interconnected networks [33]. Compared to the commercially used 0D spherical nanoparticles, titania nanostructures with higher dimensions are known to feature high accessible surface areas. Figures 1 and 2 present the structural illustrations and transmission electron microscope (TEM) images, respectively, of some representative dimensionally different nanomaterials applied for gas separation and liquid separation nanocomposite membrane.

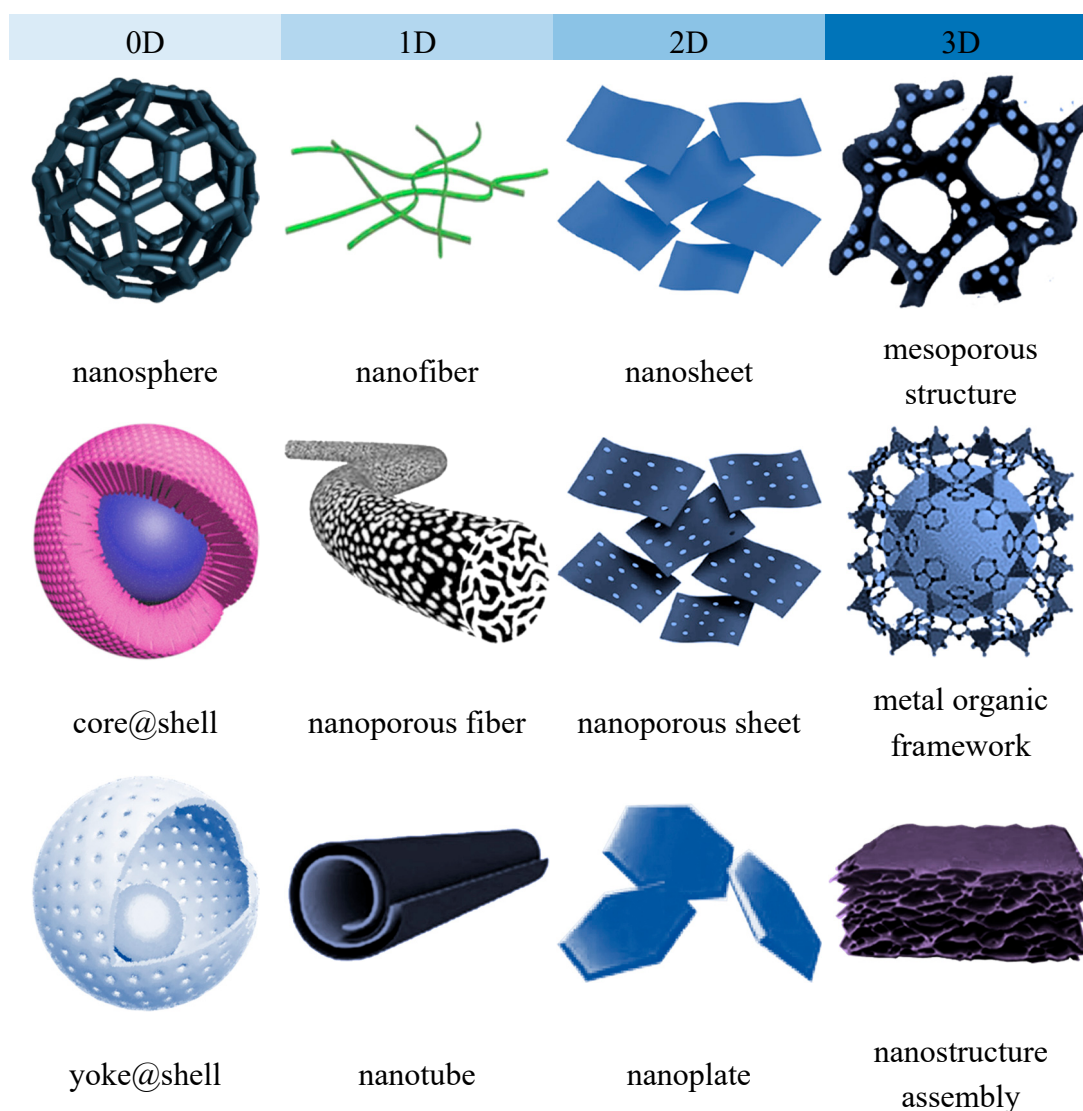


**Figure 1.** Representative illustrations of dimensionally different nanomaterials applied for gas separation and liquid separation nanocomposite membrane.

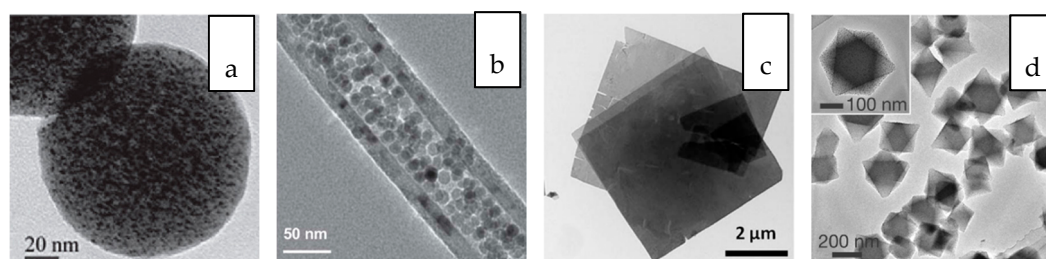


**Figure 2.** Transmission electron microscope (TEM) images of (a) 0D platinum loaded N-doped mesoporous carbon nanosphere [34], (b) 1D iron oxide nanoparticle filled carbon nanotube [35], (c) 2D metal organic framework nanosheet [36] and (d) 3D platinum loaded in between a MIL-101(Cr) core and MIL-101(Fe) shell [37].

The performance of nanocomposite membranes in liquid- and gas-separation applications depends critically upon the roles of the incorporated nanofillers. Together with many other interrelated factors, the geometry of the nanomaterial is important to dictate the ultimate performance of a nanocomposite membrane. The discrepancy in the performance of nanocomposite membranes incorporated with

structurally different but with identical chemical composition highlights the importance of material architecture. Due to this reason, the structural features should be carefully identified. These features, such as pore size and distribution, interconnectivity of pores, and interlayer spacing, play critical roles in maximizing the desired performances. The different dimensions of these nanomaterials open rooms to develop intriguing functionalities. The tunable anisotropy in transport properties and sieving properties are two aspects closely related to membrane-separation mechanisms. The understanding on the role of nanomaterials associated to their dimension and geometry should be a subject of high interest from the material science point of view. With the advances in bottom-up and top-down synthesis, nanostructures can be feasibly synthesized in various dimensions without altering their chemical composition. In this section, the classification of the nanostructures is primarily based on their most commonly known and synthesized dimensions for nanocomposite membrane applications.

### 2.1. Zero-Dimensional Nanomaterials

Zero-dimensional (0D) nanostructures are known as the forerunner of nanostructured materials. A broad range of materials can be feasibly synthesized in spherical geometry, including carbon-based materials, metals, metal oxides, semiconductors and polymers. Zero-dimensional nanostructures are the simplest building block for the design and construction of other low-dimensional materials or complex 3D nanostructures [38]. Due to the inherent structural properties of 0D nanostructures in spherical or quasi-spherical geometry, they are characterized by ultra-small size, high surface-to-volume ratio, high active edge sites per unit mass. Owing to the diameter of less than 100 nm, 0D nanoparticles exhibit edge and quantum confinement effects that are closely related to the electrical, optical, biological, mechanical behavior and other intrinsic properties of the material [39]. Most size and dimension of all 0D nanoparticles have notable effects on the physicochemical and biological properties as these factors alters the specific surface area and thermodynamic characteristics of the nanoparticles.

Nobel metallic nanoparticles are ultrafine particles with distinguishable features from the macroscopic bulk metal. Silver nanoparticles (AgNPs) are one of the most reported antibacterial nanomaterials for the preparation of biofouling-resistant nanocomposite membranes. AgNPs can be successfully utilized as antimicrobial agents, based on their multiple bacteria-killing routes [40]. Metal oxide nanoparticles such as TiO<sub>2</sub>, MgO, ZnO and Al<sub>2</sub>O<sub>3</sub> are the most common type of nanostructures used for nanocomposite membranes for both gas and liquid separation. Most of these metal oxide nanoparticles are characterized by similar physicochemical properties including large surface area, high mechanical and chemical stability. Some metal oxide nanoparticles, such as CuO [41] and ZnO [42] also exhibit strong antimicrobial activities that are comparable to that of AgNPs. The solid core of these spherical nanoparticles is impermeable so the transport of molecules across the structure has not been reported [43,44]. The surface hydrophilicity of these nanoparticles is one of the main reasons that makes them favorably used in the preparation of liquid-separation membranes. The hydrophilicity rendered by these nanoparticles improves the water flux and fouling resistant of the resultant nanocomposite membranes. On the other hand, the affinity and interaction between metal or metal oxide surface and some gas species such as CO<sub>2</sub> motivates their potential for nanocomposite membranes [45–47].

Quantum dots are luminescent semiconductor crystals with diameter ranges from 1–10 nm [48]. Carbon-based quantum dots are typically 0D spherical nanoparticles with amorphous to nanocrystalline cores [49]. Compared to the semiconductor counterpart, carbon-based quantum dots exhibit lower toxicity, higher biocompatibility, better solubility and rich chemistry. Graphene and graphene oxide (GO) quantum dots are emerging 0D nanostructures that found vast applications on account of their electronic and optical properties resulted from their large edge effects and quantum confinement [50]. They are defined as graphene or GO sheets in single or several layers with lateral dimensions less than 100 nm [51]. They inherit the unique properties of monolayer sp<sup>2</sup> carbon atoms structure and quantum effects of 0D nanostructure. Besides exhibiting attractive composition-related properties that

fit membrane application well, the nanoscale size and homogeneity of carbon-based quantum dots also ensure their good dispersibility in polar solvents and polymer matrix [52–54].

## 2.2. One-Dimensional Nanomaterials

One-dimensional (1D) nanomaterials are characterized by hollowed tubular or solid fiber structures. All 1D nanomaterials demonstrate significantly high length to diameter aspect ratio in tandem with their tubular structure. Carbon-based 1D nanomaterials, with carbon nanotubes (CNTs) as the most classical representative of this class, are the most explored 1D nanomaterials. Structurally, CNTs can be described as hollow cylindrical tubes made up from nanometer-scale rolled up sheets of graphene that are held together by Van der Waal interactions. Carbon nanowires and nanofibers which are synthesized in the form of solid rather than hollow tubes also gained similar prominence after CNT. Naturally found inorganic analogs of carbon-based tubular nanostructures are imogolite nanotubes (INTs) and halloysite nanotubes (HNTs) [55]. INTs are aluminosilicate clay minerals known as the clay counterpart of CNTs due to their similarity in terms of aspect ratio and rigidity. The single-walled imogolite nanotube consists of two-layer where the external aluminium octahedral layer is connected to the internal silica tetrahedral layer via the covalent bonding between the mutual oxygen atoms. INTs have external diameter of about 2nm and tube length that can be extended in the range of micrometer.

Also known as naturally occurring alumina-silicate clay, silicon oxygen tetrahedron and alumina oxygen octahedrons in HNT form a kaolinite-like sheet that rolls up into a tubular structure. Boron nitride nanotube (BNNT) is also a close structural analog of CNTs. The external diameter of BNNTs varies from 4 to 300 nm and the tube length is usually in the range of 5–10  $\mu\text{m}$  [56]. The tubular structure of BNNTs is similar to that of CNT, with alternating boron and nitrogen atoms, instead of carbon, arranged in a hexagonal lattice [57]. Depending on the synthesis condition, a single-walled, double-walled or multi-walled BNNT can be obtained. Because of the structural similarity, BNNTs and CNTs shared many common features including mechanical properties and thermal conductivity [58]. Fascinated by the structural properties of these 1D nanostructures, various materials particularly metal oxide, have been synthesized in tubular nanostructures. Titania nanotubes (TNT), alumina nanotubes, zinc nanotubes, just to name a few, can be prepared through well-established templating methods [59].

For the development of nanocomposite membranes, in contrast to 0D nanostructures that are known to be impermeable to water or gas molecule transports, hollowed 1D nanostructures are mainly used to facilitate fast transport, the mechanisms by which a fluidic molecule is transported in the confined tubular structure responsible to the overall permeability of the resultant nanocomposite membranes [60]. The transport and thermodynamic properties of molecules across tubular structure of 1D nanomaterial is distinguished from that in the bulk solution. This provides an opportunity to enhance water transport through the interaction between the molecules and the wall of the nano-channel walls. The ion exclusion capability of most 1D nanostructures is conferred by their permanent polarization and inner surface charge, which has in turn resulted in steric hindrance and electrostatic repulsion [61].

## 2.3. Two-Dimensional Nanomaterials

Two-dimensional (2D) nanomaterials, which have been known as the thinnest materials, are characterized by a layered structure configured as a honeycomb, governed by strong in-plane bonds and weak interlayer van der Waals forces [62]. The layered structure of 2D nanomaterial serves as the building block for the construction of nanofluidic channels that can be suitably applied for catalysis, biosensor and electrochemical energy-conversion processes. Mono- and few-layer nanosheets can be conveniently produced by physically or chemically exfoliating their van de Waals layered parent bulk counterpart. The typical example is the exfoliation of graphite to obtain graphene. Graphene is one of the most important and widely used 2D nanomaterials. After many successful implementations of graphene-enabled materials and devices, more 2D nanomaterials such as hexagonal boron nitride (hBN)

nanosheet, layered double hydroxides (LDH), layered transition metal dichalcogenides, and Mxene have been engineered.

Single-layer graphene is described as a nanosheet made from the planar arrangement of carbon atoms to form a hexagonal network. GO is described as an oxidized graphene sheet with basal planes decorated by functional groups such as carboxyl and epoxides, has been extensively used for separation processes [63]. The chemically bound functional groups expand the interlayer spacing to a desired distance, enabling selective and fast diffusion of small molecules. hBN, also known as white graphite, structurally resembles graphite hence share similar structural and physical properties with graphite [64]. Mxene is a relatively new class of 2D nanostructure composed of transition metal carbides nitrides and carbonitrides. MXene features the structure inherited from its parent MAX, which is a large family of hexagonal layered P63/mmc symmetry connected by strong metallic, ionic, and covalent bonds. Like GO, Mxene nanosheets are terminated with functional groups such as  $-H$ ,  $-O$  and  $-F$ , allowing facile post-synthesis chemical functionalization [27]. Although Mxene and graphene share many common characteristics due to similarity in their structure, Mxene is known to show better compatibility with a polymer matrix, which is advantageous for nanocomposite membrane application [65]. LDHs are commonly known as hydrotalcite-like compounds composed of layered hydroxides of divalent ( $M^{2+}$ ) and partially substituted trivalent ( $M^{3+}$ ) cations with similar ionic radii. Compared to other 2D nanostructures, the multiple metal cations in LDHs allow precise control of chemical compositions of host layers [66]. Additionally, the substitutable charge compensating anions contribute to adjustable interlayer spacing and surface functionality.

With their well-defined nanochannels and sub-nanometer pore structure, 2D materials offer precise and selective molecular separation capability. As one of the most popular choices for the development of nanocomposite membranes, the atomic-scale thickness of 2D nanostructures impart negligible transport resistance which renders fast permeation to realize high-throughput separation that is commercially attractive. Due to the structural advantage of 2D nanomaterials, pores can be directly created on the single layer nanosheets to form freestanding membranes with an ideal separation efficiency. The major technical challenge for obtaining such freestanding membranes is the difficulty of achieving uniform pore size distribution across the membrane area targeted for practical industrial applications. With more positive progress made in the synthesis and exfoliation method such as freeze-thaw exfoliation to obtain high-quality rigid crystals [67], crystalline 3D nanostructures with intrinsic nanopores have been constructed in 2D to resolve the issue related to uniform pore creation. One representative of this class of material is a 2D metal organic framework (MOF). There have been growing interest in the functionalization of 2D materials. The 2D nanochannels of sheet-like nanostructures can be easily decorated or intercalated with other functional materials to tune their physicochemical properties, impart additional functionalities or flexibility of the nanochannels to expand their application and achieve greater performances [68,69]. The interlayer composition enables structural control within the layers, where the ion or molecule selectivity and stability can be enhanced accordingly [70].

#### 2.4. Three-Dimensional Nanomaterials

In contrast to the aforementioned low-dimensional 0D, 1D and 2D nanostructures, 3D nanostructures are not characterized by a well-defined geometry. A 3D structure can be simply constructed by either connecting several building blocks that extended in all directions or combining the 2D sheet-like structure to other building blocks [71]. On the other hand, crystalline nanoporous structured materials with a rigid cage, framework, or cavities can be generally classified as 3D nanomaterials. Other examples of 3D nanostructures include aerogel, foams, fibers, pillars and layered skeletons [16,72]. In most 3D porous structures, various building blocks can be rationally engaged and synergized. By tuning the 3D porous size and introducing other functional groups within the 3D compartments, the materials can be feasibly endowed with new multifunctional properties [73,74].

The microporous structures of these porous 3D nanomaterials provide channels for molecular transports. Known for their microporous crystal-like alumino-silicates frameworks in a 3D network, zeolites have been extensively used as nanofillers, particularly for gas separation nanocomposite membranes [75,76]. The 3D arrangement of  $\text{SiO}_4$  and  $\text{AlO}_4$  tetrahedra connected by oxygen bridges forms an open framework with pores and cavities. With the uniform pore structure and a controlled channel diameter, zeolites have been proven as excellent molecular sieves that able to perform selective sorption [77] and diffusion of ions and molecules [78,79]. As zeolite micropores possess diameters that are similar to the size of many molecules, they can precisely discriminate between molecules with just a small size variation. Lately, new zeolitic materials with enhanced pore accessibility and higher mesopore surface area have been explored. These include nanozeolite with their crystal size reduced below 100 nm and hierarchical zeolites introduced with secondary porosity in the mesopore range [80].

MOFs emerged as an alternative to zeolite and other conventional mesoporous materials. MOFs are crystalline porous structure with a hybrid array of metal ions or cluster coordinated to organic ligands [81]. Due to their porosity, uniform aperture distribution and tunable pore functionalities, MOFs have been widely used for molecule discrimination via gas adsorption and separation [82]. The connectivity and interactions of the cavities with target guest molecules can be controlled by altering the organic and inorganic building blocks [83]. The zeolitic imidazole framework (ZIF) is a sub-class of MOF which has been commonly used for nanocomposite membrane [84–88]. Although the MOF has been conventionally synthesized as a isotropic bulk crystal with a 3D network, nanosheet and nanofilm MOFs are gaining popularity owing to the merits stemming from the 3D porous framework and 2D intrinsic feature [89]. The covalent organic framework (COF) is a class of crystalline porous polymer that structurally resembles MOF, but it is made of light elements such as hydrogen, boron and carbon instead of metal-based nodes and organic components in the latter [90]. The porous network structure of COF which established through the periodically extended covalent bonds is characterized by high-density and well-arranged pores as well as uniform pore size [91]. COF can be formed in eclipsed and staggered 3D structures with tunable pores. Although MOFs have been exploited in more separation applications, with more efforts made in increasing the thermal and solvent stability of COFs [92], this new class of nanostructures has also been progressively used for nanocomposite membrane preparation [93,94]. Polyhedral oligomeric silsesquioxanes (POSS) belong to the group of silsesquioxanes with a general formula  $(\text{RSiO}_{1.5})_n$ , where R is hydrogen or an organic group such as alkyl, aryl, alkylenes and their derivatives [95]. POSS has been commonly described as a 3D cage-shaped molecule composed of silica framework coordinated to multiple organic functional groups. Compared to other inorganic nanostructures, the organic linker functional groups in nanostructured hybrid inorganic-organic materials such as MOF and POSS have good affinity with polymers, hence facilitating better compatibility and interaction with polymer chains [96]. The polymer-nanofiller compatibility issues in the preparation of nanocomposite membranes can therefore be alleviated [97].

### 3. Tailoring the Dimensions of Nanostructures to the Separation Processes

The applications of various nanostructures have progressed from multiple aspects, including the fundamental understanding of water transport and molecule/ion-filler interaction through computational studies, separation performance evaluation through experimental approaches, modifications and functionalizations of nanofillers for performance enhancement. Due to their respective uniqueness and advantages originated from their structural properties and chemical composition, various nanomaterials of different dimensions have received equal attention in nanocomposite membranes. Just as the choice of the type polymer is largely dependent on the nature of the separation process, the selection of nanomaterials used for the preparation of nanocomposite membranes should also be made on the basis of their intended applications [98,99]. Tremendous efforts have been made in the preparation and performance evaluations of various forms of nanocomposite membranes. In this section, the discussion is made based on some recent exemplary work which



aims at harnessing the benefits arisen from the uniqueness of the nanostructure dimensions, instead of the benefits rendered by their chemical compositions or surface properties. Out of the vast applications of membrane processes, two niche areas where this technology has been massively explored, i.e., gas separation and liquid separation are focused.

### 3.1. Gas Separation

Dimensionally different nanostructures are introduced as a nanofiller, interlayer and coating layer of gas separation nanocomposite membranes [100]. Improved selectivity, permeability, durability and mechanical strength can be afforded by exploiting the structural advantages of many nanomaterials. In general, tubular and lamellar structures are used for facilitating the transport of gas molecules, while porous nanostructures with regular and well-defined openings or apertures are used to improve selectivity based on their molecular sieving properties [101]. 3D nanomaterials with rigid cage-like structure offer some structural advantages that are important for a gas-separation nanocomposite membrane. The last decade has witnessed tremendous efforts in developing MMM gas separation membranes based on 3D zeolite [102–104], MOF [105–107] and POSS [108–110]. In particular, MOFs exhibit a strong affinity towards CO<sub>2</sub> molecules and are able to enhance CO<sub>2</sub> solubility in the membrane hence offering excellent CO<sub>2</sub> separation performance [111,112]. Great efforts have been devoted to reduce the particle size of MOFs and zeolite to improve their compatibility with the polymer matrix [113] and to introduce building units with specific gas adsorption capacity [114,115]. When incorporated into a polymer matrix with high free volume such as glassy polyacetylenes, cage-like POSS act as rigid barrier rendering a space-filling effect to reduce the relaxation of a polymeric chain and collapse of free volume cavities [116]. The large free volume occupied by a 3D POSS can effectively suppress physical aging. However, despite the availability of open cage structures, the large free volume is not accessible to the gas molecules [117]. As no concrete evidence has been found on the transport of penetrates across it, the transport behaviour of POSS is normally regarded as a 0D nanosphere.

Realizing the intrinsic benefit of anisotropic material, there has been increasing interest over the last few years in using lamellar zeolite and MOF as the nanofiller of nanocomposite membranes [118–120]. These studies confirmed the role of 2D lamellar morphology to render a perpendicular pore orientation which can shorten diffusion paths for the desired components but increase the tortuosity of the undesired components. Kang et al. correlated the H<sub>2</sub>/CO<sub>2</sub> separation performance of MMM with the dimensional properties of a small pore MOF nanofiller, namely [Cu<sub>2</sub>(1,4-naphthalene dicarboxylate)<sub>2</sub>(1,4-diazabicyclo[2.2.2]octane)]<sub>n</sub> in the form of bulk crystal, nanocube, and nanosheet [121]. The nanosheet MOF exhibited the highest CO<sub>2</sub> uptake owing to narrow MOF channels which has provided homogeneous sorption sites for CO<sub>2</sub>. Compared to bulk crystal MOF, nanocube MOF distributed more uniformly throughout the matrix due to the reduced particle size. Nevertheless, MMM containing nanosheet MOF has exhibited the highest H<sub>2</sub> permeability and H<sub>2</sub>/CO<sub>2</sub> selectivity, as depicted in Figure 3a. The main reason lies in the partial stacking of MOF nanosheets, due to the shear force imparted during membrane casting, which serve as CO<sub>2</sub> barriers to enhance the sieving efficiency. A relatively new type of MOF, MUF-15 in bulk crystal and nanosheet geometries was introduced into a PIM-1 polymer matrix for CO<sub>2</sub> separation [122]. The MUF-15 nanosheets offered large interfacial contact area between the polymer and filler phases to enhance compatibility while interfacial voids were formed when MUF-15 bulk crystal was used. As a consequence, CO<sub>2</sub>/CH<sub>4</sub> selectivity enhancement was achieved with the former nanofiller, as depicted in Figure 3b.

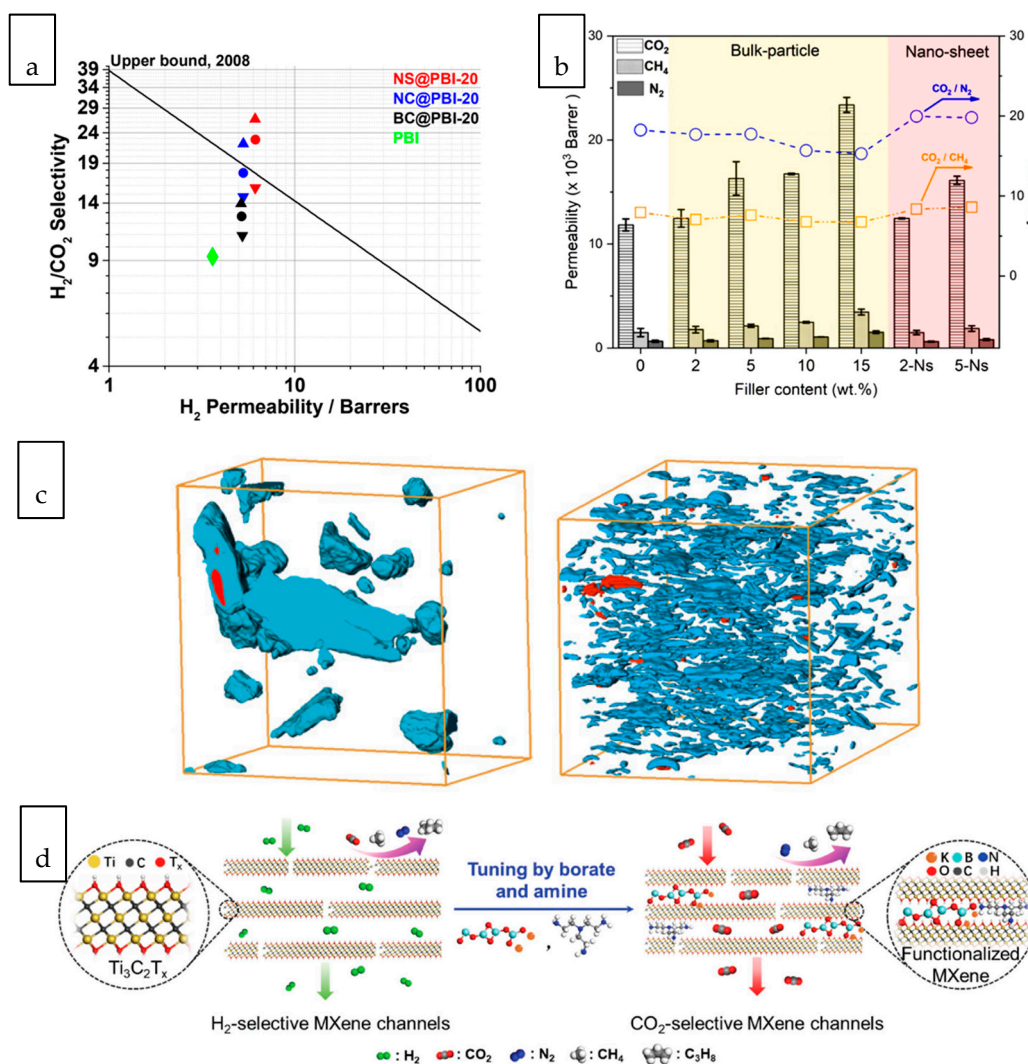


**Figure 3.** (a)  $H_2$  permeabilities versus  $H_2/CO_2$  selectivities mixed matrix membranes (MMMs) containing 20 wt% of MOFs of different dimensions benchmarked with neat polybenzimidazoles (PBI) membrane (NS: nanosheet; NC: nanocube; BC: bulk crystal) [121], (b)  $CO_2/CH_4$  separation performance of MMM incorporated with MUF-15 crystal bulk and nanosheets [122], (c) Segmented (focused ion beam- scanning electron microscope (FIB-SEM) tomograms of polyimide-based MMM containing bulk-type and nanosheet CuBDC MOF [123], (d) Schematic illustration of the interlayer functionalization of MXene to tune from a  $H_2$ -selective to  $CO_2$ -selective membrane [124].

Compared to the 3D analogue with bulkier network cage, 2D MOF can be favorable used for film formation and surface coating [125]. When used as the dispersed phase of a nanocomposite, the 2D geometry provides larger contact surface and improves the adhesion between the MOF and substrate or host matrix. It has been observed that the MOF nanosheet could disperse uniformly throughout the polymer matrix as sheet-like structures have larger contact area with polymer matrix compared to isotropic morphology. The FIB-SEM tomograms shown in Figure 3c compared the distribution of bulk crystal MOF and nanosheet MOF of same loading within the polyimide matrix [123]. A striking difference was observed where the bulk crystal left a significant fraction of unoccupied volume accompanied with non-selective voids while lamellar MOF occupied a large fraction of the volume in very uniform pattern. The surface area of nanosheets embedded in the polymer matrix was nearly 10 times greater than that of the bulk crystal counterpart of same loading of filler, which improved molecule sieving efficiency by up to 80%.

Facilitated transport membrane is important for gas separation as it enables excellent permeability and selectivity for a targeted gas through the incorporation of a carrier agent with a special affinity toward a target gas component. In this context, the 2D nanosheet and 3D nanoporous crystals are beneficial as the interlayer spacing between nanosheets and porous framework structures can readily host the carrier agents. An interesting chemical functionalization has been demonstrated by Shen et al. to tune the gas selectivity of MXene nanofilm horizontally aligned on a substrate [124]. As illustrated in Figure 3d, the interlocking of borate and polyethylenimine within the nanoconfined MXene nanosheets reduced the interlayer spacing. The chemical functionalization of CO<sub>2</sub>-philic borate which act as CO<sub>2</sub> facilitated transport carrier transformed the nanoconfined layers of Mxene from diffusion-controlled to solution-controlled channels. As a result, the membrane was tuned from a H<sub>2</sub>-selective to CO<sub>2</sub>-selective membrane. Water plays an important role in CO<sub>2</sub> facilitated transport. When incorporated into the polymer matrix, 2D nanosheets with large surface area-to-volume ratio contributes vast space to redistribute the water domain present in the humidified membrane such that water-rich domains are available throughout the matrix to facilitate the sorption of CO<sub>2</sub> [126]. The nanosheets can also effectively disrupt and induce reorientation of polymer chain packing which in turn increased gas diffusion.

In terms of the current development of polymeric membranes for gas separation, equal attention has been dedicated to both integrally skinned asymmetric membranes and thin film composite (TFC). However, for practical industrial application, TFC membranes can offer several advantages over the integrally skinned asymmetric counterpart [127]: (i) the construction of thin selective layer increases the gas permeation and overall productivity, (ii) only small amount of material is needed for the construction of the selective layer, resulting in material cost saving, (iii) independent optimization of each layer in the composite membrane. When a nanocomposite membrane is put into this context, TFN offers another significant advantage where the nanomaterials can be concentrated at the selective layer, instead of throughout the polymer matrix such as in the case of MMM, to minimize the wastage and maximize the functionalities of the selected nanomaterials [128]. Bearing in mind these structural benefits, TFN membranes are expected to be more commercial-ready compared to the MMM counterpart. As forming an intact selective layer is a top priority during the preparation of thin film membranes, the interaction of the incorporated nanomaterials and the polymer host matrix is of great importance. Bearing in mind this concern, it is not surprising that 2D nanostructures appear as the most favourable nanofiller for gas separation TFN membranes. Compared to 1D nanostructures with high aspect ratio and 3D nanostructures with rigid interconnected framework structure, 2D nanosheets can be more flexibly aligned to form highly compact layered structure or used as interlayer in the construction of TFC [129].

### 3.2. Liquid Separation

Ultrafast water transport is the ultimate goal of all liquid separation processes. Increasing membrane water permeability can potentially decrease the membrane surface area requirement and the associated costs [130]. The water permeability of membrane has also been associated with the specific energy consumption of a pressure-driven membrane process such as reverse osmosis [131]. As most commercial membrane processes have demonstrated satisfactory separation efficiencies, the application of nanocomposite membranes for liquid separation is largely related to their potential in enhancing water permeability while retaining the selectivity, primarily due to the structural features of inorganic nanomaterials. On account of their tubular or nanoporous layered structures, 1D and 2D materials are especially attractive to facilitate high water permeability across the nanocomposite membranes. As the separation mechanism of 2D nanosheets is primarily governed by the distance or tortuosity of the transport pathways, the control of lateral dimension of 2D nanofillers is useful to maximize the transport capacity [132]. By manipulating the exfoliation conditions, small- and large-flake GO nanosheets with lateral dimension of 0.03  $\mu\text{m}^2$  and 0.51  $\mu\text{m}^2$  can be obtained [133]. Using methanol as a model fluid, the nanocomposite membrane assembled with small-flake GO exhibited up to 2.7-fold higher permeance than the large-flake counterpart. The small

lateral dimension of small-flake GO enabled a less tortuous pathway which led to faster transport, as illustrated in Figure 4a. However, despite the advantage of the small-flake nanosheet, forming a homogeneous thin film of small-flake GO on top of a polymeric substrate was found to be challenging as the larger substrate pore size could not effectively retain the laminate in a localized region.

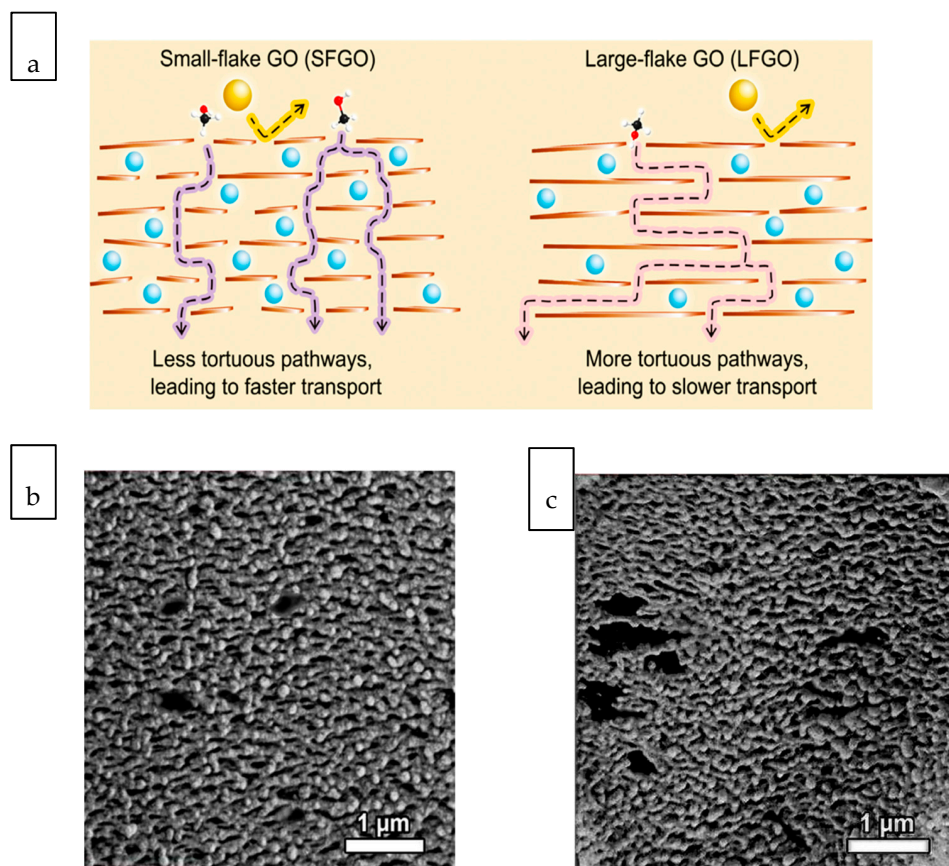


**Figure 4.** (a) Schematic illustration of solvent molecule transport pathway in small-flake graphene oxide (GO) and large-flake GO with different lateral [133], cross-sectional images of polyethersulfone (PES) support layers templated with (b) ZnO nanoparticles and (c) ZnO nanorods [134].

Nanomaterials with various dimensions have been used as pore forming templates to tailor the nanostructure of polymer substrate [135,136]. In this direct template technique, etching agents are used to remove the nanomaterials preloaded into the nanocomposite membranes, leaving templated porous structure with increased porosity and pore space connectivity. Lu et al. compared the templated porous structure of forward osmosis (FO) polysulfone (PSf) substrate formed upon the washing of 0D LDH spherule and 3D LDH flower from the nanocomposite membrane [137]. Similarly, Rastgar et al. introduced 0D ZnO nanoparticle and 2D ZnO nanorods within PES FO substrate to create secondary pores as shown in Figure 4b upon the washing-off of these nanostructures [134]. 0D spherical nanotemplate with particle size <100 nm cannot effectively interconnect the isolated pore space. The substrate templating using 3D LDH and 2D ZnO nanorod could more effectively increase the overall porosity and interconnected pore network, which in turn favoured the water diffusion through the specific channels and suppressed internal concentration polarization (ICP) in the FO membrane.

Particle size and surface area play important roles in the interaction of materials with its surrounding medium or substances [138]. These feature are especially relevant to two relatively new classes of functional nanocomposite membranes used for wastewater treatment, i.e., photocatalytic membrane and adsorptive membranes [139]. For both photocatalytic membranes and adsorptive membranes, as the photocatalyst and nanoadsorbents, respectively, cannot be wholly exposed to the

contacting medium like when they are suspended in the medium, the effective surface area available for the reaction or interaction is greatly reduced. In order to maximize the efficiency of the photocatalysts and nanoadsorbents in the nanocomposite structure, it is a priority to optimize the important features of the nanomaterials prior to their incorporation into the polymeric matrix. The effect of adsorbent dimension on its specificity toward certain types of metal ion has been evidenced. By comparing the adsorption behavior of 0D and 2D silica-based nanoadsorbents, Diab et al. observed that the 2D montmorillonite exhibited higher uptake efficiency of  $Zn^{2+}$  while 0D silica nanoparticle was more specific towards  $Cr^{3+}$  [140]. The discrepancy was attributed to the interaction of sheet-like and spherical like nanostructures with the metal ions of different ionic radii. For nanomaterials featuring antimicrobial properties, their applications in nanocomposite membrane are interesting to mitigate biofouling. Myriads of nanomaterials including AgNP and single-wall CNTs, have been incorporated into polymer matrix to afford antimicrobial properties [141,142]. Besides the chemical nature of the constituents, the intrinsic biocidal potency of the nanomaterials is also closely related to their dimensions which arise from a variety of particle sizes, shapes and aspect ratios. A comparison of the antibacterial activity of ZnO nanosphere and nanosheet over *E. coli* and *S. aureus* bacterial species evidenced that nanosphere demonstrated higher antimicrobial efficiency due to the better penetration into the cell wall of bacteria [143]. On the other hand, it has also been observed that despite having the same chemical composite, sheet-like  $RuO_2$  showed more inhibitive capability towards Gram-positive bacteria compared to its spherical counterpart [144]. The discrepancy between these studies can be attributed to the difference in their antibacterial mechanisms [145].

#### 4. Synergy of Multidimensional Hybrid Nanostructures

To further enhance the performance, more than one type of nanostructure has been simultaneously used for the construction of the membrane structure. When nanostructures with different dimensions are used, the difference in the geometric structures allows for their distinct roles in the nanocomposite membrane design. The integration of two or more nanostructures with different geometrical structures can also potentially diminish the limitation of individual component. For instances, the decoration of 1D nanoparticles on 2D materials such as graphene and MXene, which serve as the backbone, alleviate the agglomeration issues [146,147]. The interlayer of 2D materials can also be integrated with 1D nanomaterials which act as spacer to reduce the restacking tendency of nanosheets. There are two ways that two or more nanomaterials can be introduced into the nanocomposite membranes, i.e., hybridization of two or more nanomaterials as a new single entity prior to their integration with the membrane or simultaneous introduction of two or more individual nanomaterials during the membrane preparation.

The incorporation of dual nanostructure or hybrid composed of two of more dimensionally different nanostructures into gas separation membranes have been ventured by numerous studies [148–153]. Wong et al. investigated the synergistic effects of nanotubular and nanosheet structures on the formation of an interfacially polymerized polyamide layer [154]. When the dual-fillers were dispersed in their common solvent, GO nanosheets with high dispersibility served as a dispersant for the CNTs in aqueous solution hence preventing the latter from aggregating (Figure 5a,b). The deposition of nanotubes onto the basal plane of GO reduced the tendency of nanotube agglomeration. The combination of these 1D and 2D nanostructures led to the formation of a thicker and rougher polyamide layer compared to that of incorporated with single-filler. In terms of the gas separation performance, the nanocomposite membranes harnessed the high selectivity offered by CNT and the high permeability contributed by GO, hence exhibiting the optimal  $CO_2$  permeability,  $CO_2/N_2$  and  $CO_2/CH_4$  selectivity that which are 29.7%, 63.5% and 54.1% higher than that of pristine TFC membranes. By coupling 2D MXene and GO with silica microsphere and HNT, Shi et al. demonstrated the importance of identifying the right pair of nanofillers to achieve the desired synergistic dual-filler effects [155]. The Pebax-based nanocomposite membrane incorporated with GO/HNTs dual-fillers exhibited much higher  $CO_2/N_2$  selectivity than the nanocomposite membrane embedded with MXene/HNTs at the same loading. The findings stem

from the different rigidity of GO and MXene where HNTs were expected to be better wrapped by the flexible GO sheets to promote their dispersion. The preferential horizontal orientation of GO and HNTs improved the tortuosity of gas transport and hence increased the diffusivity selectivity of  $\text{CO}_2/\text{N}_2$ . In contrast to GO, MXene/ $\text{SiO}_2$  dual fillers demonstrated synergic effect that could not be observed in MXene/HNT. The dispersion of spherical  $\text{SiO}_2$  was much better than that of HNT, hence can effectively prevent the stacking of MXene.

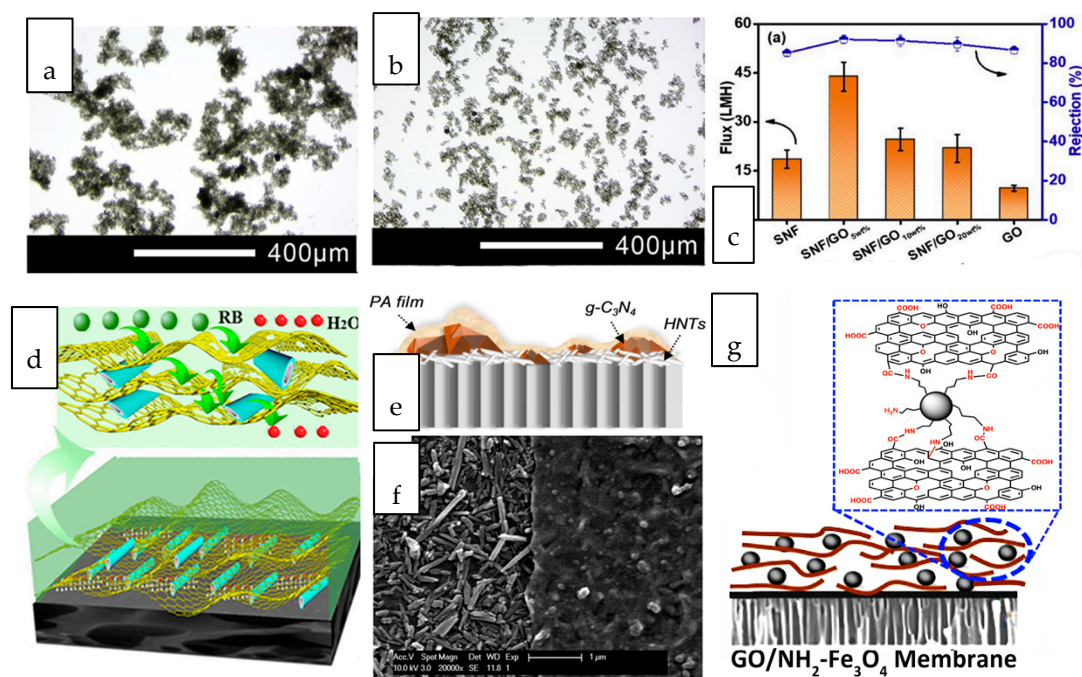


**Figure 5.** Optical images of (a) carbon nanotube (CNT) and (b) CNT/GO dual nanofiller dispersed in aqueous-based solution. (c) nanocomposite membranes incorporated with SNF/GO<sub>x</sub> exhibited drastically improved  $\text{Na}_2\text{SO}_4$  rejection and flux for the SNF, GO, and membranes [156] (d) conceptual illustration of water transport path and nanocapillary network jointly created by porous reduced graphene oxide/halloysite nanotubes (PRGO/HNTs) (RB: Reactive Black) [157] (e) Schematic illustration of cross section and (f) surface image of TFN membrane incorporated with  $g\text{-C}_3\text{N}_4$ /HNT. The left part with the PA scraped off revealed the orientation of HNT [158], (g) Schematic illustration of  $\text{NH}_2\text{-Fe}_2\text{O}_3$  intercalated GO nanosheets [159].

Various interesting combinations of nanostructures with different dimensions, including the coupling of 0D/2D nanostructures [160–169], 1D/3D nanostructures [170], 1D/2D nanostructure [171–173], 3D/2D nanostructures [174–178] have been attempted for liquid separation nanocomposite membranes. A glimpse into these works revealed the huge potential of high surface area 2D nanosheets to serve as a versatile platform for the deposition of other nanostructures while their restacking issue can be simultaneously overcome through the insertion of foreign nanostructures. The synergistic advantages of 1D silk nanofiber (SNF) and 2D GO in the nanocomposite membranes over their single counterparts when used for salt and dye separation has been demonstrated [156]. Supported on a hydrolyzed polyacrylonitrile support, the silk nanofibers intercalated between GO layers, forming organic-inorganic stackings. The flux and salt rejections of the nanocomposite membranes incorporated with SNF/GO were increased by up to 80% compared to those of incorporated with individual SNF and GO (Figure 5c). The 1D silk nanofiber interspersed between the 2D GO layers inhibited the extension of GO nanosheets thus maintaining the salt rejection capability. The additional space created by the SNF interspersed between the GO nanosheet layers led to an optimal increase in the membrane free volume, creating more flow path for water transport. Sheet-like porous reduced graphene oxide (PRGO) and tubular halloysite nanotubes (HNT) were used to create a continuous sandwich-like water channel for efficient dye

removal [157]. The driving force induced during solvent-evaporation coating facilitated the movement of HNT to the interlayer spacing of two adjacent PRGO sheets, forming a network of nanocapillaries as illustrated in Figure 5d. 2D graphitic carbon nitride ( $g\text{-C}_3\text{N}_4$ ) and 1D HNTs were co-deposited onto a substrate through vacuum filtration prior to interfacial polymerization of polyamide selective layer [158]. Due to the distinct dimension of these nanostructures, the tubular HNTs inclined to horizontally oriented on the substrate surface to act as an interlayer, while  $g\text{-C}_3\text{N}_4$  particles scattered within the PA layer as a porous nanofiller, as revealed in the surface morphology shown in Figure 5e,f. The intrinsic nanopores across the lamellar  $g\text{-C}_3\text{N}_4$  and nanotubular structure of HNTs provided additional water transport pathways, which eventually led to elevated water permeability up to  $20.5 \text{ L}\cdot\text{m}^{-2}\cdot\text{h}^{-1}\cdot\text{bar}^{-1}$  while maintaining the salt rejection capability.

Zero-dimensional nanoparticles are favourably used as intercalating agent for sheet-like nanostructures due to their good dispersibility throughout the interlayer spacing. Amine functionalized  $\text{Fe}_3\text{O}_4$  nanospheres were intercalated within the interlayer of GO (Figure 5g) to enlarge the interlayer spacing and improve the water stability of the GO-coated membranes [159]. The nanocomposite membranes augmented by  $\text{Fe}_2\text{O}_3/\text{GO}$  exhibited a water flux of up to  $78 \text{ L}\cdot\text{m}^{-2}\cdot\text{h}^{-1}$  in dye/salt separation, which was nearly 5 times greater than that with single GO. Three-dimensional nanostructures have been increasingly used for intercalation of nanosheets. The precisely controlled framework and cage-like structures of many 3D nanomaterials can offer additional sieving capabilities without hindering the passage of water molecules. Unlike impermeable nanostructures, the opening of nanoporous crystals with 3D channels can increase the porosity and introduce more nanofluidic channels [179]. By incorporating UiO-66 nanoporous crystals with sub-nano aperture size into the reduced graphene oxide (rGO) laminates, the result exhibited 15 times higher water permeability than the nanocomposite membrane incorporated with rGO without compromising the dye removal efficiency [180]. The improvement was attributed to the abundant adsorption sites and extra water paths rendered by the 3D/2D hybrid.

## 5. Anisotropy and Orientations of Nanostructures

Nanostructured materials with high aspect ratios or extended lateral dimensions are endowed with exciting physicochemical properties that are radically different from those isotropic counterparts. However, these unique direction-dependent properties can only be harnessed if the orientation of these anisotropic nanostructures is taken into consideration. The preferable orientation of the nanomaterials not only may exhibit properties superior to the disordered counterparts, but also maximize the anisotropic properties of the nanomaterials to approach their ideal performance [181,182]. As the alignment of 1D and 2D nanostructures in their preferable direction is important to fit their purpose, the directional alignment of anisotropic nanomaterials in the nanocomposite membranes should be given particular attention. In the majority of cases, the incorporated nanomaterials are assumed to be randomly orientated and uniformly dispersed within the polymer matrix. The enhancement in separation properties are generally discussed based on the overall physicochemical properties contributed by the nanomaterials, rather than the advantages arisen from the structure or dimension of the selected materials.

Tubular and sheet-like nanomaterials, when oriented in different directions within the polymer matrix, result in different gas transport behaviors. As depicted in Figure 6a, for composite membranes with a relatively thick selective layer, GO nanosheets aligned perpendicular to the membrane surface facilitated the diffusion of gas molecules through the interlayer spacing of nanosheets while that aligned parallel to the membrane surface lengthens the pathway for the passage of gas molecules although the gas molecules still preferably transported through the GO interlayer spacing [183]. However, despite this ideal orientation, the practicability of the membrane should also be taken into consideration. Formation of thin ( $\sim 1 \mu\text{m}$ ) selectively layer that is preferable for a practical separation process may not favour the vertically or randomly oriented GO nanosheets considering the defects and voids created. Zhang et al. aligned GO horizontally in the thin PEBAX selective layer (Figure 6b)

by taking the advantage of shear effects during dip-coating process [184]. Although the tortuosity of the gas transport pathway has been increased upon the addition of GO, the parallel-aligned GO laminates provide size-selective and fast gas transport channels without creating defects within the selective layer. Compared to the randomly oriented and neat polymeric membrane, the nanocomposite membrane with parallel-aligned GO demonstrated improved CO<sub>2</sub> permeance without compromising the CO<sub>2</sub>/N<sub>2</sub> selectivity.

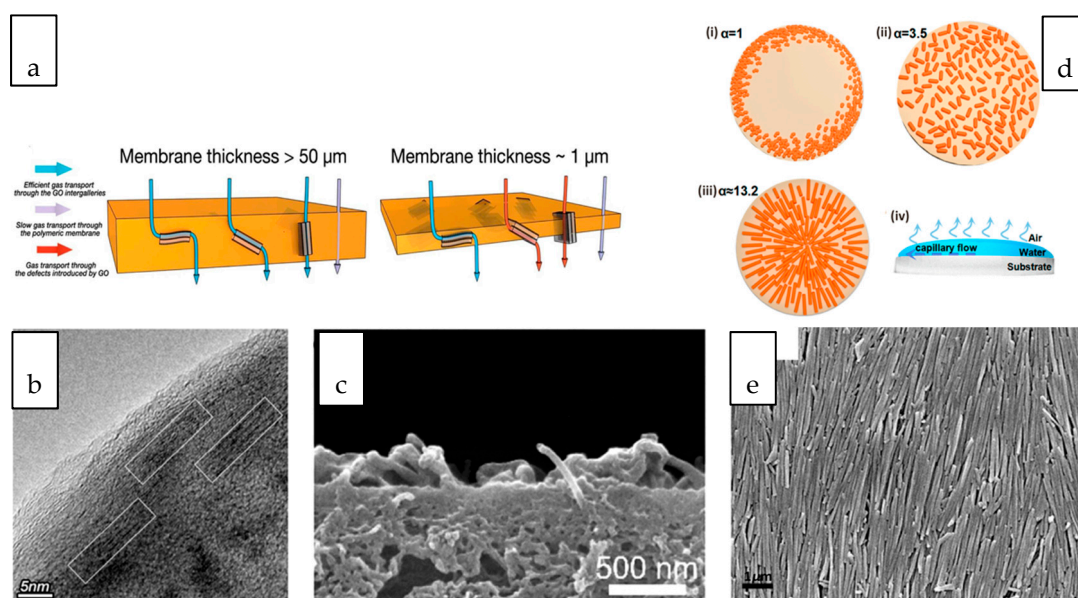


**Figure 6.** (a) Schematic illustration of gas transport pathway across membrane with different thickness [184] (b) Cross-sectional image of GO nanosheets aligned at parallel direction with membrane surface [184] (c) Cross-sectional images of nanocomposite membranes showing the protrusion of the tubes [185]. (d) Schematic illustration of nanomaterials with different aspect ratio ( $\alpha$ ) (i) coffee-ring effect observed in isotropic nanostructures, (ii) uniform distribution of ellipsoid nanostructures (iii) orientation of nanotubular nanostructure, (iv) evaporation deposition of nanomaterials on a substrate [186]. (e) Surface image of oriented HNT [186].

When 1D CNT emerged as one of the most studied nanofillers for nanocomposite membranes, the astonishing transport behaviour modelled from vertically aligned CNT has evoked several breakthrough efforts in preparing nanocomposite membranes with vertically-aligned CNT. The vertical alignment has been realized through an infiltration technique which involves the wetting and infiltration of the vertically aligned CNT array by the chosen polymer solution to fill up the inter-tube gaps [187]. The approach may not be favourable for large-scale preparation but it has stimulated more interest in exploring other scalable technique to accomplish the alignment of CNT within nanocomposite membranes. The magnetic and electrical responsiveness of CNT makes the application of a unidirectionally magnetic and electrical field a promising technique for facile nanotube alignment [188]. Polyamide NF TFC membrane with electrically-aligned CNTs that were vertically spanning from polysulfone substrate to polyamide selective layer demonstrated a several-fold increase in the water flux [185]. However, by considering the thickness of membrane and the length of CNT which normally ranges from a few microns to a few centimeters, the length of vertically aligned CNT must be carefully controlled to avoid protrusion of the tubes, as shown in Figure 6c [185]. In another study, the orientation of aluminogermanate imogolite nanotube to the direction of the water flow path within the polyamide layer of TFC membrane was evidenced as the primary factor contributing to the increased specific water flux [189]. The improvement was attributed to the reduction in the length of the water passage across the thin film.



Solvent evaporation is a common technique employed for the formation of a thin film embedded with nanofillers [190]. The deposition and distribution of nanostructures during evaporation is a dimension-dependent process. The coffee-ring effect refers to the deposition of the suspended particulate in a ring-like fashion, mainly observed for the deposition of isotropic materials, such as the nanosphere [191]. Figure 6d compares the deposition patterns of nanostructures of different aspect ratios [186]. It is observed that the deposition of nanostructures with anisotropic geometry through evaporation can significantly deform the interfaces and produce strong interparticle capillary interactions. These deformations are responsible for the elimination of the coffee-ring effect where uniform deposition of the nanostructures can be achieved. The uniform distribution and alignment is more significant with the increasing aspect ratio of the nanostructure, as evidenced in the orientation of HNT on the polyacrylonitrile substrate through evaluation (Figure 6e) [186].

## 6. Gaps and Perspectives

Developing a high-performance membrane would largely heighten the separation performances and sustainability of a membrane process. The nanocomposite membrane is currently at the forefront of membrane research and development, owing to its unparalleled physicochemical properties capable of resolving the underlying issues of conventional membranes. It is without any doubt that nanomaterials offer a bridge between atomic characteristics and macroscopic devices or materials. In parallel with the advancement in nanocomposite membranes, there is a need to look into the architecture and design of the material. For nanocomposite membrane development, the focus has been largely placed on exploring various fascinating nanomaterials to break the boundaries between laboratory attempts and commercial application. The main challenge of current material selection for the development of a high-performance nanocomposite membranes is that there are too many potential candidates available. Dozens of new materials of various geometrical structures and their allotropes have emerged in the past few years. With many more anticipated to exist, the selection of material obviously cannot be fulfilled by simply trying thousands of existing materials. A strong integration of theories and the understanding of the characteristics of materials and their resulting properties is crucial to promote good matching and design of new materials that suit their applications well. A true understanding the material properties is a gateway for achieving more significant breakthroughs in material developments. Additionally, the membrane development cycle can be effectively shortened while the benefits can be fully optimized.

Albeit the fact that great progress has been made in exploring the potential of new nanomaterials to enhance the performance of membranes for liquid and gas separations, there is still plenty of room for improvement. Along with the emergence of more exciting nanomaterials that can be potentially used for nanocomposite membranes, it is worth putting more effort into understanding and refining the properties of the existing materials. There are three common ways to tune the properties of nanostructures, i.e., by altering the chemical composition, surface functionalization and structure/morphology. These alterations not only lead to the corresponding changes in their physicochemical properties, but also functionalities that are responsible for their applications. While the research topics related to surface functionalization have been an evergreen favourite, the importance of understanding the role of dimension of the nanostructures in designing high-performance nanocomposite membranes should not be overlooked.

The versatility of altering the dimension of a performance-proof nanostructure to furnish other desired properties is an interesting strength to intensify the applicability of these nanostructures for the preparation of nanocomposite membranes. By taking carbon-based nanomaterials as an example, the majority of the carbon allotropes are engineered and artificially synthesized in the laboratory. Therefore, the nanostructures enjoy high versatility for further modification, in both in situ or post-synthesis stages. This flexibility stimulates more innovation in nanomaterial synthesis and modifications. The better control and understanding in a top-down exfoliation strategy or bottom-up assembly methods allow the alteration of nanostructure dimension, from what it is commonly known

to be. One vivid example is the conversion of a 3D rigid MOF to 2D flexible network to address the limitations of the former [89]. The diffusivity and accessibility of molecules to the active sites of the MOF can be improved without compromising the chemical functionality as well as chemical stability demonstrated by the 3D analogue. Such a fascinating 2D material has been recently explored for nanocomposite membranes where their superior properties arising from the 2D structure are evidenced from the improved performance. Interestingly, 2D graphene-based nanostructures have been architected into 3D macrostructures such as in the form of graphene hydrogel and graphene sponge [192]. A three-dimensional microporous graphene network has been topologically synthesized with interconnected channels of zeolite as a template on account of their high porosity, large specific surface area and light weight [193]. The structural advantages have been witnessed in some applications, including for oil/water separation and gas separation. Although these materials are still not common for the development of nanocomposite membranes, the anisotropic properties of graphene-based materials deserve further attentions. Metal oxide nanoparticles which have been conventionally synthesized as 0D spherical nanostructures have also been increasingly explored in their 2D structures [26].

It is important to unlock the full potential of nanomaterials by matching their unique structural characteristics with the applications of the resultant nanocomposite membranes. For instance, the orientation of anisotropic nanofillers should not be neglected if they are intended for rendering mechanical reinforcement. Similarly, for many nanostructures that are targeted for facilitating molecular transport, more studies should be directed to more in depth understanding of the transport pathways within these materials. With more examples demonstrating the importance of directional alignment of anisotropic nanomaterials in affecting molecular transport pathways, more attention should be placed on looking into the possible ways to maximize the benefits of these nanomaterials. This review does not intend to delve in the alignment techniques but rather to pinpoint the necessity of putting more emphasis on understanding the effects of nanomaterial orientations on the behavior of the nanomaterials. This is especially important for 1D and 2D nanostructures that are intended for fast molecular transport. It is undeniably challenging to precisely tune the orientation of these nanostructured particularly when processed over a large membrane area. The molecular transport across a nanocomposite membrane is very different from that of polymeric or inorganic membranes as it integrates the motion of fluid through and around the nanostructure as well as across the polymeric or inorganic structure. In many experimental studies, the effects of nanofiller orientation on the molecule flow path across the nanocomposite membranes have been neglected. Although this topic remains a great challenge, closing the gaps will be a key step towards performance optimization.

The hybrid of multidimensional nanostructures is an interesting route to magnify the structural advantages of the nanostructures and to mitigate the issues related to their processing such as dispersion and compatibility. Functional nanostructures with enhanced properties can be synergistically achieved from two or multiple components in the resultant hybrid. The synergistic effects revealed the infinite possibilities to fine tune the properties and functions of nanomaterials through judicious pairing of nanostructures. Compared to the confined tubular structure of 1D and spherical hollowless 0D structures, 2D nanosheets create a more versatile platform for the insertion of foreign materials between the two adjacent nanosheets. The current work majorly focuses on the binary hybrid of nanostructures of the same dimension or different dimensions. Ternary or quaternary hybrid nanostructures with properties that are expected to surpass that of the binary should be given more attention in future research. While synergistic effects are generally observed in most dual-filler or hybrid systems, both experimental and molecular simulation studies are needed to provide further clarifications and insights regarding the role of each component. By taking the MOF/GO hybrid as an example, although it has been agreed that the water flux enhancement was mainly attributed to the increase in the GO interlayer spacing as a result of MOF intercalation, a recent computational study has pointed out that the high water permeability can only be effectively achieved with high loading of MOF [194]. Such finding highlights the potential of exploiting the selective adsorption capacity, rather than the water channel, of MOF to augment the membrane performances. It is also rational to point out

that, although enhanced separation performances have been reported with the co-existence of two or more fillers in the nanocomposite membranes, most descriptions are made based on the conceptual interactions between the hybridized components. Direct evidence of their interactions such as the arrangement of tubular nanomaterials between the interlayer spacing of sheet-like nanostructures has not been fully found with the existing characterization tools.

Confusion arises when attempts are made to distinguish the roles of nanomaterials proffered by their geometries, physical properties and chemical compositions. While it is unnecessary to isolate the multiple factors that influence the nanomaterial properties, based on the exemplary findings discussed in this review, the dimension of these nanostructures has a disregarded role in determining the functions of the nanomaterials. Admittedly, for some nanomaterials, the unique physical properties induced from the dimensional advantages have not been truly exploited in the preparation of nanocomposite membranes. For instance, the quantum size effects associated to 0D nanostructures has marginal significance in the enhancement of nanocomposite membranes. However, the surface properties related to their chemical composition such as surface charges of metal oxide nanoparticles, antibacterial properties of AgNP and surface functionalities of GO quantum dots play more important roles in tailoring the properties of the resultant nanocomposite membranes. It would be a meaningful line of research if further exploration can be made to further verify the dimension-dependent properties of the nanomaterials. A direct comparison of the structural properties and separation performance of nanocomposite membranes prepared with the same material composition and experimental condition, but of different dimensions, will provide a clear indication of the roles of material dimensions. For examples, the characterization and performance evaluation of a series of photocatalytic membranes prepared with 0D titania nanoparticle, 1D titania nanosheet, 2D titania nanotube and 3D titania nanoshell would provide useful information regarding the interactions of these multidimensional nanostructures with the polymer matrix, the trend in textural, morphological and optical properties as well as the correlations of these factors with the photocatalytic and filtration performances of the resultant nanocomposite membranes. Such comparison not only gives a unified view concerning the effects of dimension, but will also be helpful for screening and selecting the optimal nanostructure at the preliminary stage.

## 7. Conclusions

In this review, we have discussed the roles of nanostructure dimensions, specifically those based on their applications in nanocomposite membranes dedicated to gas separation and water reclamation. Despite the undeniable benefits offered by nanomaterials in the resultant nanocomposite membrane, there are many fundamental aspects which can be looked into. One of these is the role of the material dimensions. The classifications of nanomaterials based on their dimension serves as a useful guideline to screen a wide range of nanomaterials based on their structural properties. Nevertheless, proper inspection of their unique dimensional features is of utmost importance to avoid the mismatch between the nanomaterials and the purpose they serve when incorporated into the nanocomposite membranes. The discussions based on the exemplary works in gas and liquid nanocomposite membranes provided further insights into this aspect. The research gaps and perspectives on these lines have also been identified, some of which are a great challenge and remain to be further explored. The insights reached in the article can be extended beyond the materials that have been explored thus far. Nanocomposite membranes used for other purposes, for instance fuel cell and biomedical applications, will also become relevant if the roles of nanofillers are clearly defined. With many successful attempts acting as a driving force, it can be envisaged that the research and development of nanocomposite membranes in the field of separation will continue to expand in the coming decade.

**Author Contributions:** Writing—original draft preparation, P.S.G.; writing—review and editing, K.C.W.; supervision, A.F.I. All authors have read and agreed to the published version of the manuscript.

**Funding:** This research was funded by the Ministry of Higher Education, Malaysia under the Fundamental Research Grant Scheme, grant number 5F005.

**Conflicts of Interest:** The authors declare no conflict of interest. The funders had no role in the design of the study; in the collection, analyses, or interpretation of data; in the writing of the manuscript; or in the decision to publish the results.

## References

1. Iulianelli, A.; Drioli, E. Membrane engineering: Latest advancements in gas separation and pre-treatment processes, petrochemical industry and refinery, and future perspectives in emerging applications. *Fuel Process. Technol.* **2020**, *206*, 106464. [[CrossRef](#)]
2. Yusuf, A.; Sodiq, A.; Giwa, A.; Eke, J.; Pikuda, O.; De Luca, G.; Di Salvo, J.L.; Chakraborty, S. A review of emerging trends in membrane science and technology for sustainable water treatment. *J. Clean. Prod.* **2020**, *266*, 121867. [[CrossRef](#)]
3. Wang, Y.; Seo, B.; Wang, B.; Zamel, N.; Jiao, K.; Adroher, X.C. Fundamentals, materials, and machine learning of polymer electrolyte membrane fuel cell technology. *Energy AI* **2020**, *1*, 100014. [[CrossRef](#)]
4. Zheng, X.; Zhang, Z.; Yu, D.; Chen, X.; Cheng, R.; Min, S.; Wang, J.; Xiao, Q.; Wang, J. Overview of membrane technology applications for industrial wastewater treatment in China to increase water supply. *Resour. Conserv. Recycl.* **2015**, *105*, 1–10. [[CrossRef](#)]
5. Matteucci, S.; Chakraborty, D. Risk management for industrial adoption of membrane technology. *Curr. Opin. Chem. Eng.* **2020**, *28*, 112–117. [[CrossRef](#)]
6. Koros, W.J.; Zhang, C. Materials for next-generation molecularly selective synthetic membranes. *Nat. Mater.* **2017**, *16*, 289–297. [[CrossRef](#)]
7. Cheng, X.Q.; Wang, Z.X.; Jiang, X.; Li, T.; Lau, C.H.; Guo, Z.; Ma, J.; Shao, L. Towards sustainable ultrafast molecular-separation membranes: From conventional polymers to emerging materials. *Prog. Mater. Sci.* **2018**, *92*, 258–283. [[CrossRef](#)]
8. Anjum, M.; Miandad, R.; Waqas, M.; Gehany, F.; Barakat, M. Remediation of wastewater using various nano-materials. *Arab. J. Chem.* **2019**, *12*, 4897–4919. [[CrossRef](#)]
9. Rao, R.; Pint, C.L.; Islam, A.E.; Weatherup, R.S.; Hofmann, S.; Meshot, E.R.; Wu, F.; Zhou, C.; Dee, N.; Amama, P.B.; et al. Carbon Nanotubes and Related Nanomaterials: Critical Advances and Challenges for Synthesis toward Mainstream Commercial Applications. *ACS Nano* **2018**, *12*, 11756–11784. [[CrossRef](#)] [[PubMed](#)]
10. Saleem, H.; Zaidi, S.J. Nanoparticles in reverse osmosis membranes for desalination: A state of the art review. *Desalination* **2020**, *475*, 114171. [[CrossRef](#)]
11. Nasir, A.; Masood, F.; Yasin, T.; Hameed, A. Progress in polymeric nanocomposite membranes for wastewater treatment: Preparation, properties and applications. *J. Ind. Eng. Chem.* **2019**, *79*, 29–40. [[CrossRef](#)]
12. Zhang, J.; Xin, Q.; Li, X.; Yun, M.; Xu, R.; Wang, S.; Li, Y.; Lin, L.; Ding, X.; Ye, H.; et al. Mixed matrix membranes comprising aminosilane-functionalized graphene oxide for enhanced CO<sub>2</sub> separation. *J. Membr. Sci.* **2019**, *343–354*. [[CrossRef](#)]
13. Chung, T.-S.; Jiang, L.Y.; Li, Y.; Kulprathipanja, S. Mixed matrix membranes (MMMs) comprising organic polymers with dispersed inorganic fillers for gas separation. *Prog. Polym. Sci.* **2007**, *32*, 483–507. [[CrossRef](#)]
14. Xu, G.-R.; Wang, S.-H.; Zhao, H.-L.; Wu, S.-B.; Xu, J.-M.; Li, L.; Liu, X.-Y. Layer-by-layer (LBL) assembly technology as promising strategy for tailoring pressure-driven desalination membranes. *J. Membr. Sci.* **2015**, *493*, 428–443. [[CrossRef](#)]
15. Zhao, D.L.; Japip, S.; Zhang, Y.; Weber, M.; Maletzko, C.; Chung, T.-S. Emerging thin-film nanocomposite (TFN) membranes for reverse osmosis: A review. *Water Res.* **2020**, *173*, 115557. [[CrossRef](#)]
16. Saleh, T.A. Nanomaterials: Classification, properties, and environmental toxicities. *Environ. Technol. Innov.* **2020**, *20*, 101067. [[CrossRef](#)]
17. Tiwari, J.N.; Tiwari, R.N.; Kim, K.S. Zero-dimensional, one-dimensional, two-dimensional and three-dimensional nanostructured materials for advanced electrochemical energy devices. *Prog. Mater. Sci.* **2012**, *57*, 724–803. [[CrossRef](#)]
18. Khan, W.S.; Asmatulu, R. Nanotechnology Emerging Trends, Markets, and Concerns. *Nanotechnol. Saf.* **2013**, *1–16*. [[CrossRef](#)]

19. Zhang, N.; Qi, W.; Huang, L.; Jiang, E.; Bao, J.; Zhang, X.; An, B.; He, G. Review on structural control and modification of graphene oxide-based membranes in water treatment: From separation performance to robust operation. *Chin. J. Chem. Eng.* **2019**, *27*, 1348–1360. [[CrossRef](#)]
20. Ali, S.; Rehman, S.A.U.; Luan, H.-Y.; Farid, M.U.; Huang, H. Challenges and opportunities in functional carbon nanotubes for membrane-based water treatment and desalination. *Sci. Total. Environ.* **2019**, *646*, 1126–1139. [[CrossRef](#)]
21. Janakiram, S.; Ahmadi, M.; Dai, Z.; Ansaloni, L.; Deng, L. Performance of Nanocomposite Membranes Containing 0D to 2D Nanofillers for CO<sub>2</sub> Separation: A Review. *Membranes* **2018**, *8*, 24. [[CrossRef](#)] [[PubMed](#)]
22. Ang, E.Y.; Toh, W.; Yeo, J.; Lin, R.; Liu, Z.; Geethalakshmi, K.; Ng, T.Y. A review on low dimensional carbon desalination and gas separation membrane designs. *J. Membr. Sci.* **2020**, *598*, 117785. [[CrossRef](#)]
23. Esfahani, M.R.; Aktij, S.A.; Dabaghian, Z.; Firouzjaei, M.D.; Rahimpour, A.; Eke, J.; Escobar, I.C.; Abolhassani, M.; Greenlee, L.F.; Esfahani, A.R.; et al. Nanocomposite membranes for water separation and purification: Fabrication, modification, and applications. *Sep. Purif. Technol.* **2019**, *213*, 465–499. [[CrossRef](#)]
24. Liu, M.; Gurr, P.A.; Fu, Q.; Webley, P.; Qiao, G.G. Two-dimensional nanosheet-based gas separation membranes. *J. Mater. Chem. A* **2018**, *6*, 23169–23196. [[CrossRef](#)]
25. Liu, Y. Beyond graphene oxides: Emerging 2D molecular sieve membranes for efficient separation. *Chin. J. Chem. Eng.* **2019**, *27*, 1257–1271. [[CrossRef](#)]
26. Safarpour, M.; Arefi-Oskoui, S.; Khataee, A. A review on two-dimensional metal oxide and metal hydroxide nanosheets for modification of polymeric membranes. *J. Ind. Eng. Chem.* **2020**, *82*, 31–41. [[CrossRef](#)]
27. Ihsanullah, I. MXenes (two-dimensional metal carbides) as emerging nanomaterials for water purification: Progress, challenges and prospects. *Chem. Eng. J.* **2020**, *388*, 124340. [[CrossRef](#)]
28. Shen, X.; Zheng, Q.; Sadighi, Z. Rational design of two-dimensional nanofillers for polymer nanocomposites toward multifunctional applications. *Prog. Mater. Sci.* **2021**, *115*, 100708. [[CrossRef](#)]
29. Huang, L.; Lin, H. Engineering Sub-Nanometer Channels in Two-Dimensional Materials for Membrane Gas Separation. *Membranes* **2018**, *8*, 100. [[CrossRef](#)]
30. Fu, S.-Y.; Sun, Z.; Huang, P.; Li, Y.-Q.; Hu, N. Some basic aspects of polymer nanocomposites: A critical review. *Nano Mater. Sci.* **2019**, *1*, 2–30. [[CrossRef](#)]
31. Nasir, S.; Hussein, M.Z.; Zainal, Z.; Yusof, N.A. Carbon-Based Nanomaterials/Allotropes: A Glimpse of Their Synthesis, Properties and Some Applications. *Materials* **2018**, *11*, 295. [[CrossRef](#)] [[PubMed](#)]
32. Tiwari, S.K.; Kumar, V.; Huczko, A.; Oraon, R.; De Adhikari, A.; Nayak, G.C. Magical Allotropes of Carbon: Prospects and Applications. *Crit. Rev. Solid State Mater. Sci.* **2016**, *41*, 257–317. [[CrossRef](#)]
33. Fattakhova-Rohlfing, D.; Zaleska, A.; Bein, T. Three-Dimensional Titanium Dioxide Nanomaterials. *Chem. Rev.* **2014**, *114*, 9487–9558. [[CrossRef](#)] [[PubMed](#)]
34. Yang, T.; Ling, H.; Lamonier, J.-F.; Jaroniec, M.; Huang, J.; Monteiro, M.J.; Liu, J. A synthetic strategy for carbon nanospheres impregnated with highly monodispersed metal nanoparticles. *NPG Asia Mater.* **2016**, *8*, e240. [[CrossRef](#)]
35. Baaziz, W.; Liu, X.; Florea, I.; Bégin-Colin, S.; Pichon, B.; Ulhaq, C.; Ersen, O.; Soria-Sánchez, M.; Zafeiratos, S.; Janowska, I.; et al. Carbon nanotube channels selectively filled with monodispersed Fe<sub>3-x</sub>O<sub>4</sub> nanoparticles. *J. Mater. Chem. A* **2013**, *1*, 13853. [[CrossRef](#)]
36. Zhang, B.; Luo, Y.; Kanyuck, K.; Saenz, N.; Reed, K.; Zavaliy, P.; Mowery, J.D.; Bauchan, G. Facile and template-free solvothermal synthesis of mesoporous/macroporous metal-organic framework nanosheets. *RSC Adv.* **2018**, *8*, 33059–33064. [[CrossRef](#)]
37. Zhao, M.; Yuan, K.; Wang, Y.; Li, G.; Guo, J.; Gu, L.; Hu, W.; Zhao, H.; Tang, Z. Metal-organic frameworks as selectivity regulators for hydrogenation reactions. *Nat. Cell Biol.* **2016**, *539*, 76–80. [[CrossRef](#)]
38. Ma, Y.; Li, H.; Bridges, D.; Peng, P.; Lawrie, B.J.; Feng, Z.; Hu, A. Zero-dimensional to three-dimensional nanojoining: Current status and potential applications. *RSC Adv.* **2016**, *6*, 75916–75936. [[CrossRef](#)]
39. Liu, Y.; Huang, H.; Cao, W.; Mao, B.; Liu, Y.; Kang, Z. Advances in carbon dots: From the perspective of traditional quantum dots. *Mater. Chem. Front.* **2020**, *4*, 1586–1613. [[CrossRef](#)]
40. Pryshchepa, O.; Pomastowski, P.; Buszewski, B. Silver nanoparticles: Synthesis, investigation techniques, and properties. *Adv. Colloid Interface Sci.* **2020**, *284*, 102246. [[CrossRef](#)]
41. Akintelu, S.A.; Folorunso, A.S.; Folorunso, F.A.; Oyebamiji, A.K. Green synthesis of copper oxide nanoparticles for biomedical application and environmental remediation. *Heliyon* **2020**, *6*, e04508. [[CrossRef](#)] [[PubMed](#)]

42. Mahamuni-Badiger, P.P.; Patil, P.M.; Badiger, M.V.; Patel, P.R.; Gadgil, B.S.T.-; Pandit, A.; Bohara, R.A. Biofilm formation to inhibition: Role of zinc oxide-based nanoparticles. *Mater. Sci. Eng. C* **2020**, *108*, 110319. [[CrossRef](#)] [[PubMed](#)]
43. Fan, C.; Chi, H.; Zhang, C.; Cui, R.; Lu, W.; Yuan, M.; Qin, Y. Effect of multiscale structure on the gas barrier properties of poly(lactic acid)/Ag nanocomposite films. *Polym. Adv. Technol.* **2019**, *30*, 1709–1715. [[CrossRef](#)]
44. Najafi, M.; Sadeghi, M.; Bolverdi, A.; Chenar, M.P.; Pakizeh, M. Gas permeation properties of cellulose acetate/silica nanocomposite membrane. *Adv. Polym. Technol.* **2017**, *37*, 2043–2052. [[CrossRef](#)]
45. Sanaeepur, H.; Ahmadi, R.; Ebadi Amooghin, A.; Ghanbari, D. A novel ternary mixed matrix membrane containing glycerol-modified poly(ether-block-amide) (Pebax 1657)/copper nanoparticles for CO<sub>2</sub> separation. *J. Membr. Sci.* **2019**, *573*, 234–246. [[CrossRef](#)]
46. Azizi, N.; Mohammadi, T.; Behbahani, R.M. Synthesis of a new nanocomposite membrane (PEBAX-1074/PEG-400/TiO<sub>2</sub>) in order to separate CO<sub>2</sub> from CH<sub>4</sub>. *J. Nat. Gas Sci. Eng.* **2017**, *37*, 39–51. [[CrossRef](#)]
47. Azizi, N.; Mohammadi, T.; Behbahani, R.M. Synthesis of a PEBAX-1074/ZnO nanocomposite membrane with improved CO<sub>2</sub> separation performance. *J. Energy Chem.* **2017**, *26*, 454–465. [[CrossRef](#)]
48. Shirke, Y.M.; Abou-Elanwar, A.M.; Choi, W.-K.; Lee, H.; Hong, S.U.; Lee, H.K.; Jeon, J.-D. Influence of nitrogen/phosphorus-doped carbon dots on polyamide thin film membranes for water vapor/N<sub>2</sub> mixture gas separation. *RSC Adv.* **2019**, *9*, 32121–32129. [[CrossRef](#)]
49. Wang, Y.; Hu, A. Carbon quantum dots: Synthesis, properties and applications. *J. Mater. Chem. C* **2014**, *2*, 6921–6939. [[CrossRef](#)]
50. Chung, S.; Revia, R.A.; Zhang, M. Graphene Quantum Dots and Their Applications in Bioimaging, Biosensing, and Therapy. *Adv. Mater.* **2019**, *1904362*, 1–26. [[CrossRef](#)]
51. Song, X.; Zhou, Q.; Zhang, T.; Xu, H.; Wang, Z. Pressure-assisted preparation of graphene oxide quantum dot-incorporated reverse osmosis membranes: Antifouling and chlorine resistance potentials. *J. Mater. Chem. A* **2016**, *4*, 16896–16905. [[CrossRef](#)]
52. Zhao, D.L.; Chung, T.-S. Applications of carbon quantum dots (CQDs) in membrane technologies: A review. *Water Res.* **2018**, *147*, 43–49. [[CrossRef](#)]
53. He, Y.; Zhao, D.L.; Chung, T.-S. Na<sup>+</sup> functionalized carbon quantum dot incorporated thin-film nanocomposite membranes for selenium and arsenic removal. *J. Membr. Sci.* **2018**, *564*, 483–491. [[CrossRef](#)]
54. Salestan, S.K.; Seyedpour, S.F.; Rahimpour, A.; Shamsabadi, A.A.; Tiraferri, A.; Soroush, M. Molecular Dynamics Insights into the Structural and Water Transport Properties of a Forward Osmosis Polyamide Thin-Film Nanocomposite Membrane Modified with Graphene Quantum Dots. *Ind. Eng. Chem. Res.* **2020**, *59*, 14447–14457. [[CrossRef](#)]
55. Lisuzzo, L.; Cavallaro, G.; Lazzara, G.; Milioto, S.; Parisi, F.; Stetsyshyn, Y. Stability of Halloysite, Imogolite, and Boron Nitride Nanotubes in Solvent Media. *Appl. Sci.* **2018**, *8*, 1068. [[CrossRef](#)]
56. Kalay, S.; Yilmaz, Z.; Sen, O.; Emanet, M.; Kazanc, E.; Çulha, M. Synthesis of boron nitride nanotubes and their applications. *Beilstein J. Nanotechnol.* **2015**, *6*, 84–102. [[CrossRef](#)] [[PubMed](#)]
57. Golberg, D.; Bando, Y.; Huang, Y.; Terao, T.; Mitome, M.; Tang, C.; Zhi, C. Boron Nitride Nanotubes and Nanosheets. *ACS Nano* **2010**, *4*, 2979–2993. [[CrossRef](#)]
58. Kim, J.H.; Pham, T.V.; Hwang, J.H.; Kim, C.S.; Kim, M.J. Boron nitride nanotubes: Synthesis and applications. *Nano Converg.* **2018**, *5*, 1–13. [[CrossRef](#)]
59. Ogihara, H.; Masahiro, S.; Nodasaka, Y.; Ueda, W. Synthesis, characterization and formation process of transition metal oxide nanotubes using carbon nanofibers as templates. *J. Solid State Chem.* **2009**, *182*, 1587–1592. [[CrossRef](#)]
60. Son, M.; Novotny, V.; Choi, H. Thin-film nanocomposite membrane with vertically embedded carbon nanotube for forward osmosis. *Desalin. Water Treat.* **2016**, *57*, 26670–26679. [[CrossRef](#)]
61. Paineau, E. Imogolite Nanotubes: A Flexible Nanoplatform with Multipurpose Applications. *Appl. Sci.* **2018**, *8*, 1921. [[CrossRef](#)]
62. Zhang, H. Ultrathin Two-Dimensional Nanomaterials. *ACS Nano* **2015**, *9*, 9451–9469. [[CrossRef](#)] [[PubMed](#)]
63. Lyu, J.; Wen, X.; Kumar, U.; You, Y.; Chen, V.; Joshi, R.K. Separation and purification using GO and r-GO membranes. *RSC Adv.* **2018**, *8*, 23130–23151. [[CrossRef](#)]

64. Zhang, K.; Feng, Y.; Wang, F.; Yang, Z.; Wang, J. Two dimensional hexagonal boron nitride (2D-hBN): Synthesis, properties and applications. *J. Mater. Chem. C* **2017**, *5*, 11992–12022. [[CrossRef](#)]
65. Li, J.; Li, J.; Van Der Bruggen, B. An MXene-based membrane for molecular separation. *Environ. Sci. Nano* **2020**, *7*, 1289–1304. [[CrossRef](#)]
66. Lu, P.; Liu, Y.; Zhou, T.; Wang, Q.; Li, Y. Recent advances in layered double hydroxides (LDHs) as two-dimensional membrane materials for gas and liquid separations. *J. Membr. Sci.* **2018**, *567*, 89–103. [[CrossRef](#)]
67. Wang, X.; Chi, C.; Zhang, K.; Qian, Y.; Gupta, K.M.; Kang, Z.; Jiang, J.; Zhao, D. Reversed thermo-switchable molecular sieving membranes composed of two-dimensional metal-organic nanosheets for gas separation. *Nat. Commun.* **2017**, *8*, 14460. [[CrossRef](#)]
68. Dou, H.; Xu, M.; Jiang, B.; Wen, G.; Zhao, L.; Wang, B.; Yu, A.; Bai, Z.; Sun, Y.; Zhang, L.; et al. Bioinspired Graphene Oxide Membranes with Dual Transport Mechanisms for Precise Molecular Separation. *Adv. Funct. Mater.* **2019**, *29*, 1–10. [[CrossRef](#)]
69. Guan, G.; Han, M. Functionalized Hybridization of 2D Nanomaterials. *Adv. Sci.* **2019**, *6*, 1901837. [[CrossRef](#)]
70. Ye, J.; Zhang, B.; Gu, Y.; Yu, M.; Wang, D.; Wu, J.; Li, J. Tailored Graphene Oxide Membranes for the Separation of Ions and Molecules. *ACS Appl. Nano Mater.* **2019**, *2*, 6611–6621. [[CrossRef](#)]
71. Xu, Y.; Xu, Y.; Gao, C.; Duan, X. Three-dimensional macro-structures of two-dimensional nanomaterials. *Chem. Soc. Rev.* **2016**, *45*, 5541–5588. [[CrossRef](#)]
72. Hasanpour, M.; Hatami, M. Application of three dimensional porous aerogels as adsorbent for removal of heavy metal ions from water/wastewater: A review study. *Adv. Colloid Interface Sci.* **2020**, *284*, 102247. [[CrossRef](#)] [[PubMed](#)]
73. Li, S.; Jiang, X.; Yang, X.; Bai, Y.; Shao, L. Nanoporous framework “reservoir” maximizing low-molecular-weight enhancer impregnation into CO<sub>2</sub>-philic membranes for highly-efficient CO<sub>2</sub> capture. *J. Membr. Sci.* **2019**, 278–285. [[CrossRef](#)]
74. Yang, S.; Karve, V.V.; Justin, A.; Kochetygov, I.; Espín, J.; Asgari, M.; Trukhina, O.; Sun, D.T.; Peng, L.; Queen, W.L. Enhancing MOF performance through the introduction of polymer guests. *Coord. Chem. Rev.* **2021**, *427*, 213525. [[CrossRef](#)]
75. Bastani, D.; Esmaili, N.; Asadollahi, M. Polymeric mixed matrix membranes containing zeolites as a filler for gas separation applications: A review. *J. Ind. Eng. Chem.* **2013**, *19*, 375–393. [[CrossRef](#)]
76. Kosinov, N.N.; Gascon, J.; Kapteijn, F.; Hensen, E.J. Recent developments in zeolite membranes for gas separation. *J. Membr. Sci.* **2016**, *499*, 65–79. [[CrossRef](#)]
77. Krachumram, S.; Chanapattharapol, K.C.; Kamonsutthipaijit, N. Synthesis and characterization of NaX-type zeolites prepared by different silica and alumina sources and their CO<sub>2</sub> adsorption properties. *Microporous Mesoporous Mater.* **2021**, *310*, 110632. [[CrossRef](#)]
78. Borjigin, B.; Liu, L.; Yu, L.; Xu, L.; Zhao, C.; Wang, J. Influence of incorporating beta zeolite nanoparticles on water permeability and ion selectivity of polyamide nanofiltration membranes. *J. Environ. Sci.* **2020**, *98*, 77–84. [[CrossRef](#)]
79. Dai, Q.; Lu, W.; Zhao, Y.; Zhang, H.; Zhu, X.; Li, X. Advanced scalable zeolite “ions-sieving” composite membranes with high selectivity. *J. Membr. Sci.* **2020**, *595*, 117569. [[CrossRef](#)]
80. Přeč, J.; Pizarro, P.; Serrano, D.P.; Čejka, J. From 3D to 2D zeolite catalytic materials. *Chem. Soc. Rev.* **2018**, *47*, 8263–8306. [[CrossRef](#)]
81. Liu, H.; Zhang, M.; Zhao, H.; Jiang, Y.; Liu, G.; Gao, J. Enhanced dispersibility of metal-organic frameworks (MOFs) in the organic phase via surface modification for TFN nanofiltration membrane preparation. *RSC Adv.* **2020**, *10*, 4045–4057. [[CrossRef](#)]
82. Yao, J.; Wang, H. Zeolitic imidazolate framework composite membranes and thin films: Synthesis and applications. *Chem. Soc. Rev.* **2014**, *43*, 4470–4493. [[CrossRef](#)]
83. Wang, T.; Lin, E.; Peng, Y.-L.; Chen, Y.; Cheng, P.; Zhang, Z. Rational design and synthesis of ultramicroporous metal-organic frameworks for gas separation. *Coord. Chem. Rev.* **2020**, *423*, 213485. [[CrossRef](#)]
84. Li, M.-P.; Zhang, X.; Zhang, H.; Liu, W.-L.; Huang, Z.-H.; Xie, F.; Ma, X.-H.; Xu, Z.-L. Hydrophilic yolk-shell ZIF-8 modified polyamide thin-film nanocomposite membrane with improved permeability and selectivity. *Sep. Purif. Technol.* **2020**, *247*, 116990. [[CrossRef](#)]

85. Beh, J.; Ooi, B.; Lim, J.; Ng, E.; Mustapa, H. Development of high water permeability and chemically stable thin film nanocomposite (TFN) forward osmosis (FO) membrane with poly(sodium 4-styrenesulfonate) (PSS)-coated zeolitic imidazolate framework-8 (ZIF-8) for produced water treatment. *J. Water Process. Eng.* **2020**, *33*, 101031. [[CrossRef](#)]
86. Lee, T.H.; Oh, J.Y.; Hong, S.P.; Lee, J.M.; Roh, S.M.; Kim, S.H.; Park, H.B. ZIF-8 particle size effects on reverse osmosis performance of polyamide thin-film nanocomposite membranes: Importance of particle deposition. *J. Membr. Sci.* **2019**, *23*–33. [[CrossRef](#)]
87. Japip, S.; Erifin, S.; Chung, T.-S. Reduced thermal rearrangement temperature via formation of zeolitic imidazolate framework (ZIF)-8-based nanocomposites for hydrogen purification. *Sep. Purif. Technol.* **2019**, *212*, 965–973. [[CrossRef](#)]
88. Zheng, W.; Ding, R.; Yang, K.; Dai, Y.; Yan, X.; He, G. ZIF-8 nanoparticles with tunable size for enhanced CO<sub>2</sub> capture of Pebax based MMMs. *Sep. Purif. Technol.* **2019**, *214*, 111–119. [[CrossRef](#)]
89. Zheng, W.; Tsang, C.-S.; Lee, L.Y.S.; Wong, K.-Y. Two-dimensional metal-organic framework and covalent-organic framework: Synthesis and their energy-related applications. *Mater. Today Chem.* **2019**, *12*, 34–60. [[CrossRef](#)]
90. Fan, H.; Gu, J.; Meng, H.; Knebel, A.; Caro, J. High-Flux Membranes Based on the Covalent Organic Framework COF-LZU1 for Selective Dye Separation by Nanofiltration. *Angew. Chem. Int. Ed.* **2018**, *57*, 4083–4087. [[CrossRef](#)]
91. Yuan, S.; Li, X.; Zhu, J.; Zhang, G.; Van Puyvelde, P.; Van Der Bruggen, B. Covalent organic frameworks for membrane separation. *Chem. Soc. Rev.* **2019**, *48*, 2665–2681. [[CrossRef](#)] [[PubMed](#)]
92. Xu, L.; Xu, J.; Shan, B.; Wang, X.; Gao, C. TpPa-2-incorporated mixed matrix membranes for efficient water purification. *J. Membr. Sci.* **2017**, *526*, 355–366. [[CrossRef](#)]
93. Li, C.; Li, S.; Tian, L.; Zhang, J.; Su, B.; Hu, M.Z. Covalent organic frameworks (COFs)-incorporated thin film nanocomposite (TFN) membranes for high-flux organic solvent nanofiltration (OSN). *J. Membr. Sci.* **2019**, *572*, 520–531. [[CrossRef](#)]
94. Gonzales, R.R.; Park, M.J.; Bae, T.-H.; Yang, Y.; Abdel-Wahab, A.; Phuntsho, S.; Shon, H.K. Melamine-based covalent organic framework-incorporated thin film nanocomposite membrane for enhanced osmotic power generation. *Desalination* **2019**, *459*, 10–19. [[CrossRef](#)]
95. Wu, J.; Mather, P.T. POSS Polymers: Physical Properties and Biomaterials Applications. *Polym. Rev.* **2009**, *49*, 25–63. [[CrossRef](#)]
96. Caro, J. Are MOF membranes better in gas separation than those made of zeolites? *Curr. Opin. Chem. Eng.* **2011**, *1*, 77–83. [[CrossRef](#)]
97. Wu, T.; Prasetya, N.; Li, K. Recent advances in aluminium-based metal-organic frameworks (MOF) and its membrane applications. *J. Membr. Sci.* **2020**, *615*, 118493. [[CrossRef](#)]
98. Wen, Y.; Yuan, J.; Ma, X.; Wang, S.; Liu, Y. Polymeric nanocomposite membranes for water treatment: A review. *Environ. Chem. Lett.* **2019**, *17*, 1539–1551. [[CrossRef](#)]
99. Yin, J.; Deng, B. Polymer-matrix nanocomposite membranes for water treatment. *J. Membr. Sci.* **2015**, *479*, 256–275. [[CrossRef](#)]
100. Liang, C.Z.; Chung, T.-S.; Lai, J.-Y. A review of polymeric composite membranes for gas separation and energy production. *Prog. Polym. Sci.* **2019**, *97*, 101141. [[CrossRef](#)]
101. Zhu, J.; Yuan, S.; Wang, J.; Zhang, Y.; Tian, M.; Van Der Bruggen, B. Microporous organic polymer-based membranes for ultrafast molecular separations. *Prog. Polym. Sci.* **2020**, *110*, 101308. [[CrossRef](#)]
102. Rezaei-DashtArzhandi, M.; Ismail, A.; Goh, P.S.; Azelee, I.W.; Abbasgholipourghadim, M.; Rehman, G.U.; Matsuura, T. Zeolite ZSM5-Filled PVDF Hollow Fiber Mixed Matrix Membranes for Efficient Carbon Dioxide Removal via Membrane Contactor. *Ind. Eng. Chem. Res.* **2016**, *55*, 12632–12643. [[CrossRef](#)]
103. Lee, P.S.; Hong, D.-Y.; Cha, G.-Y.; An, H.; Moon, S.-Y.; Seong, M.; Chang, B.-J.; Lee, J.S.; Kim, J.-H. Mixed matrix membranes incorporated with three-dimensionally ordered mesopore imprinted (3DOM-i) zeolite. *Sep. Purif. Technol.* **2019**, *210*, 29–37. [[CrossRef](#)]
104. Zhao, J.; Xie, K.; Liu, L.; Liu, M.; Qiu, W.; Webley, P.A. Enhancing plasticization-resistance of mixed-matrix membranes with exceptionally high CO<sub>2</sub>/CH<sub>4</sub> selectivity through incorporating ZSM-25 zeolite. *J. Membr. Sci.* **2019**, *583*, 23–30. [[CrossRef](#)]



105. Ahmad, M.Z.; Peters, T.A.; Konnertz, N.M.; Visser, T.; Téllez, C.; Coronas, J.; Fila, V.; de Vos, W.M.; Benes, N.E. High-pressure CO<sub>2</sub>/CH<sub>4</sub> separation of Zr-MOFs based mixed matrix membranes. *Sep. Purif. Technol.* **2020**, *230*, 115858. [[CrossRef](#)]
106. Ozen, H.A.; Ozturk, B. Gas separation characteristic of mixed matrix membrane prepared by MOF-5 including different metals. *Sep. Purif. Technol.* **2019**, *211*, 514–521. [[CrossRef](#)]
107. Akbari, A.; Karimi-Sabet, J.; Ghoreishi, S.M. Matrimid® 5218 based mixed matrix membranes containing metal organic frameworks (MOFs) for helium separation. *Chem. Eng. Process. Process. Intensif.* **2020**, *148*, 107804. [[CrossRef](#)]
108. Kinoshita, Y.; Wakimoto, K.; Gibbons, A.H.; Isfahani, A.P.; Kusuda, H.; Sivaniah, E.; Ghalei, B. Enhanced PIM-1 membrane gas separation selectivity through efficient dispersion of functionalized POSS fillers. *J. Membr. Sci.* **2017**, *539*, 178–186. [[CrossRef](#)]
109. Guerrero, G.; Hägg, M.B.; Kignelman, G.; Simon, C.; Peters, T.; Rival, N.; Denonville, C. Investigation of amino and amidino functionalized Polyhedral Oligomeric Silsesquioxanes (POSS®) nanoparticles in PVA-based hybrid membranes for CO<sub>2</sub>/N<sub>2</sub> separation. *J. Membr. Sci.* **2017**, *544*, 161–173. [[CrossRef](#)]
110. Konnertz, N.; Ding, Y.; Harrison, W.J.; Budd, P.M.; Schönhal, A.; Böhning, M. Molecular mobility and gas transport properties of nanocomposites based on PIM-1 and polyhedral oligomeric phenethyl-silsesquioxanes (POSS). *J. Membr. Sci.* **2017**, *529*, 274–285. [[CrossRef](#)]
111. Ghanbari, T.; Abnisa, F.; Daud, W.M.A.W. A review on production of metal organic frameworks (MOF) for CO<sub>2</sub> adsorption. *Sci. Total. Environ.* **2020**, *707*, 135090. [[CrossRef](#)] [[PubMed](#)]
112. Kazemi, S.; Safarifard, V. Carbon dioxide capture in MOFs: The effect of ligand functionalization. *Polyhedron* **2018**, *154*, 236–251. [[CrossRef](#)]
113. Li, W.; Chuah, C.Y.; Kwon, S.; Goh, K.; Wang, R.; Na, K.; Bae, T.-H. Nanosizing zeolite 5A fillers in mixed-matrix carbon molecular sieve membranes to improve gas separation performance. *Chem. Eng. J. Adv.* **2020**, *2*, 100016. [[CrossRef](#)]
114. Ishaq, S.; Tamime, R.; Bilad, M.R.; Khan, A.L. Mixed matrix membranes comprising of polysulfone and microporous Bio-MOF-1: Preparation and gas separation properties. *Sep. Purif. Technol.* **2019**, *210*, 442–451. [[CrossRef](#)]
115. Chen, W.; Zhang, Z.; Hou, L.; Yang, C.; Shen, H.; Yang, K.; Wang, Z. Metal-organic framework MOF-801/PIM-1 mixed-matrix membranes for enhanced CO<sub>2</sub>/N<sub>2</sub> separation performance. *Sep. Purif. Technol.* **2020**, *250*, 117198. [[CrossRef](#)]
116. Khosravi, A.; Vatani, A.; Mohammadi, T. Application of polyhedral oligomeric silsesquioxane to the stabilization and performance enhancement of poly(4-methyl-2-pentyne) nanocomposite membranes for natural gas conditioning. *J. Appl. Polym. Sci.* **2017**, *134*, 45158. [[CrossRef](#)]
117. Iyer, P.; Iyer, G.; Coleman, M.R. Gas transport properties of polyimide–POSS nanocomposites. *J. Membr. Sci.* **2010**, *358*, 26–32. [[CrossRef](#)]
118. Akbari, A.; Karimi-Sabet, J.; Ghoreishi, S.M. Polyimide based mixed matrix membranes incorporating Cu-BDC nanosheets for impressive helium separation. *Sep. Purif. Technol.* **2020**, *253*, 117430. [[CrossRef](#)]
119. Shete, M.; Kumar, P.; Bachman, J.E.; Ma, X.; Smith, Z.P.; Xu, W.; Mkhoyan, K.A.; Long, J.R.; Tsapatsis, M. On the direct synthesis of Cu(BDC) MOF nanosheets and their performance in mixed matrix membranes. *J. Membr. Sci.* **2018**, *549*, 312–320. [[CrossRef](#)]
120. Sabetghadam, A.; Liu, X.; Gottmer, S.; Chu, L.; Gascon, J.; Kapteijn, F. Thin mixed matrix and dual layer membranes containing metal-organic framework nanosheets and Polyactive™ for CO<sub>2</sub> capture. *J. Membr. Sci.* **2019**, *226–235*. [[CrossRef](#)]
121. Kang, Z.; Peng, Y.; Hu, Z.; Qian, Y.; Chi, C.; Yeo, L.Y.; Tee, L.; Zhao, D. Mixed matrix membranes composed of two-dimensional metal–organic framework nanosheets for pre-combustion CO<sub>2</sub> capture: A relationship study of filler morphology versus membrane performance. *J. Mater. Chem. A* **2015**, *3*, 20801–20810. [[CrossRef](#)]
122. Yinab, H.; Alkasa, A.; Zhanga, Y.; Zhangc, Y.; Telfer, S.G. Mixed matrix membranes (MMMs) using an emerging metal-organic framework (MUF-15) for CO<sub>2</sub> separation. *J. Membr. Sci.* **2020**, *609*, 118245. [[CrossRef](#)]
123. Rodenas, T.; Luz, I.; Prieto, G.; Seoane, B.; Miro, H.; Corma, A.; Kapteijn, F.; Xamena, F.X.L.I.; Gascon, J. Metal–organic framework nanosheets in polymer composite materials for gas separation. *Nat. Mater.* **2014**, *14*, 48–55. [[CrossRef](#)] [[PubMed](#)]

124. Shen, J.; Liu, G.; Ji, Y.; Liu, Q.; Cheng, L.; Guan, K.; Zhang, M.; Liu, G.; Xiong, J.; Yang, J.; et al. 2D MXene Nanofilms with Tunable Gas Transport Channels. *Adv. Funct. Mater.* **2018**, *28*, 1–13. [[CrossRef](#)]
125. Dhakshinamoorthy, A.; Asiri, A.M.; Garcia, H. 2D Metal–Organic Frameworks as Multifunctional Materials in Heterogeneous Catalysis and Electro/Photocatalysis. *Adv. Mater.* **2019**, *31*, e1900617. [[CrossRef](#)]
126. Janakiram, S.; Espejo, J.L.M.; Yu, X.; Ansaloni, L.; Deng, L. Facilitated transport membranes containing graphene oxide-based nanoplatelets for CO<sub>2</sub> separation: Effect of 2D filler properties. *J. Membr. Sci.* **2020**, *616*, 118626. [[CrossRef](#)]
127. Castro-Muñoz, R.; Agrawal, K.V.; Coronas, J. Ultrathin permselective membranes: The latent way for efficient gas separation. *RSC Adv.* **2020**, *10*, 12653–12670. [[CrossRef](#)]
128. Wong, K.C.; Goh, P.S.; Ismail, A. Thin film nanocomposite: The next generation selective membrane for CO<sub>2</sub> removal. *J. Mater. Chem. A* **2016**, *4*, 15726–15748. [[CrossRef](#)]
129. Wen, Y.; Zhang, X.; Li, X.; Wang, Z.; Tang, C.Y. Metal–Organic Framework Nanosheets for Thin-Film Composite Membranes with Enhanced Permeability and Selectivity. *ACS Appl. Nano Mater.* **2020**, *3*, 9238–9248. [[CrossRef](#)]
130. Okamoto, Y.; Lienhard, J.H. How RO membrane permeability and other performance factors affect process cost and energy use: A review. *Desalination* **2019**, *470*, 114064. [[CrossRef](#)]
131. Cohen-Tanugi, D.; McGovern, R.K.; Dave, S.H.; Lienhard, J.H.; Grossman, J.C. Quantifying the potential of ultra-permeable membranes for water desalination. *Energy Environ. Sci.* **2014**, *7*, 1134–1141. [[CrossRef](#)]
132. Saraswat, V.; Jacobberger, R.M.; Ostrander, J.S.; Hummell, C.L.; Way, A.J.; Arnold, M.S.; Zanni, M.T.; Arnold, M.S. Invariance of Water Permeance through Size-Differentiated Graphene Oxide Laminates. *ACS Nano* **2018**, *12*, 7855–7865. [[CrossRef](#)]
133. Nie, L.; Goh, K.; Wang, Y.; Lee, J.; Huang, Y.; Karahan, H.E.; Zhou, K.; Guiver, M.D.; Bae, T.-H. Realizing small-flake graphene oxide membranes for ultrafast size-dependent organic solvent nanofiltration. *Sci. Adv.* **2020**, *6*, eaaz9184. [[CrossRef](#)] [[PubMed](#)]
134. Shakeri, A.; Bozorg, A.; Shakeri, A. Novel Dimensionally Controlled Nanopore Forming Template in Forward Osmosis Membranes. *Environ. Sci. Technol.* **2018**, *52*, 2704–2716. [[CrossRef](#)]
135. Kellenberger, C.; Luechinger, N.A.; Lamprou, A.; Rossier, M.; Grass, R.N.; Stark, W.J. Soluble nanoparticles as removable pore templates for the preparation of polymer ultrafiltration membranes. *J. Membr. Sci.* **2012**, *387*, 76–82. [[CrossRef](#)]
136. Li, J.; Liu, Q.; Li, X.; Liu, Y.; Xie, J. Template-Assisted Fabrication of Thin-Film Composite Forward-Osmosis Membrane with Controllable Internal Concentration Polarization. *Ind. Eng. Chem. Res.* **2016**, *55*, 5327–5334. [[CrossRef](#)]
137. Lu, P.; Li, W.; Yang, S.; Wei, Y.; Zhang, Z.; Li, Y.-S. Layered double hydroxides (LDHs) as novel macropore-templates: The importance of porous structures for forward osmosis desalination. *J. Membr. Sci.* **2019**, *585*, 175–183. [[CrossRef](#)]
138. Huangfu, X.; Xu, Y.; Liu, C.; He, Q.; Ma, J.; Ma, C.; Huang, R. A review on the interactions between engineered nanoparticles with extracellular and intracellular polymeric substances from wastewater treatment aggregates. *Chemosphere* **2019**, *219*, 766–783. [[CrossRef](#)]
139. Nasir, A.M.; Goh, P.; Abdullah, M.S.; Ng, B.C.; Ismail, A.; Cheer, N.B. Adsorptive nanocomposite membranes for heavy metal remediation: Recent progresses and challenges. *Chemosphere* **2019**, *232*, 96–112. [[CrossRef](#)]
140. Diab, M.; Attia, N.F.; Attia, A.; El-Shahat, M. Green Synthesis of Cost-Effective and Efficient Nanoadsorbents Based on Zero and Two Dimensional Nanomaterials for Zn<sup>2+</sup> and Cr<sup>3+</sup> Removal from Aqueous Solutions. *Synth. Met.* **2020**, *265*, 116411. [[CrossRef](#)]
141. Shukla, A.K.; Alam, J.; Ansari, M.A.; Alhoshan, M.; Alam, M.; Kaushik, A. Selective ion removal and antibacterial activity of silver-doped multi-walled carbon nanotube / polyphenylsulfone nanocomposite membranes. *Mater. Chem. Phys.* **2019**, *233*, 102–112. [[CrossRef](#)]
142. Al Aani, S.; Gomez, V.; Wright, C.J.; Hilal, N. Fabrication of antibacterial mixed matrix nanocomposite membranes using hybrid nanostructure of silver coated multi-walled carbon nanotubes. *Chem. Eng. J.* **2017**, *326*, 721–736. [[CrossRef](#)]
143. Singh, R.; Verma, K.; Patyal, A.; Sharma, I.; Barman, P.; Sharma, D. Nanosheet and nanosphere morphology dominated photocatalytic & antibacterial properties of ZnO nanostructures. *Solid State Sci.* **2019**, *89*, 1–14. [[CrossRef](#)]

144. Ananth, A.; Dharaneedharan, S.; Gandhi, M.S.; Heo, M.-S.; Mok, Y.S. Novel RuO<sub>2</sub> nanosheets—Facile synthesis, characterization and application. *Chem. Eng. J.* **2013**, *223*, 729–736. [[CrossRef](#)]
145. Baranwal, A.; Srivastava, A.; Kumar, P.; Bajpai, V.K.; Maurya, P.K.; Chandra, P. Prospects of Nanostructure Materials and Their Composites as Antimicrobial Agents. *Front. Microbiol.* **2018**, *9*, 422. [[CrossRef](#)]
146. Yinab, J.; Zhanb, F.; Jiao, T.; Dengb, H.; Zoua, G.; Baic, Z.; Zhangb, Q.; Peng, Q. Highly efficient catalytic performances of nitro compounds via hierarchical PdNPs-loaded MXene/polymer nanocomposites synthesized through electrospinning strategy for wastewater treatment. *Chin. Chem. Lett.* **2020**, *31*, 992–995. [[CrossRef](#)]
147. Yanga, W.; Hua, W.; Zhanga, J.; Wang, W.; Caib, R.; Pana, M.; Huanga, C.; Chenb, X.; Yanc, B.; Zenga, H. Tannic acid/Fe<sup>3+</sup> functionalized magnetic graphene oxide nanocomposite with high loading of silver nanoparticles as ultra-efficient catalyst and disinfectant for wastewater treatment. *Chem. Eng. J.* **2021**, *405*, 126629. [[CrossRef](#)]
148. Li, X.; Ma, L.; Zhang, H.; Wang, S.; Jiang, Z.; Guo, R.; Wu, H.; Cao, X.; Yang, J.; Wang, B. Synergistic effect of combining carbon nanotubes and graphene oxide in mixed matrix membranes for efficient CO<sub>2</sub> separation. *J. Membr. Sci.* **2015**, *479*, 1–10. [[CrossRef](#)]
149. Ahmad, N.; Noh, A.M.; Leo, C.; Ahmad, A. CO<sub>2</sub> removal using membrane gas absorption with PVDF membrane incorporated with POSS and SAPO-34 zeolite. *Chem. Eng. Res. Des.* **2017**, *118*, 238–247. [[CrossRef](#)]
150. Galve, A.; Sieffert, D.; Staudt, C.; Ferrando, M.; Güell, C.; Téllez, C.; Coronas, J. Combination of ordered mesoporous silica MCM-41 and layered titanosilicate JDF-L1 fillers for 6FDA-based copolyimide mixed matrix membranes. *J. Membr. Sci.* **2013**, *431*, 163–170. [[CrossRef](#)]
151. Jamil, N.; Othman, N.H.; Alias, N.H.; Shahrudin, M.Z.; Roslan, R.A.; Lau, W.J.; Ismail, A.F. Mixed matrix membranes incorporated with reduced graphene oxide (rGO) and zeolitic imidazole framework-8 (ZIF-8) nanofillers for gas separation. *J. Solid State Chem.* **2019**, *270*, 419–427. [[CrossRef](#)]
152. Lia, X.; Yua, S.; Lia, K.; Mab, C.; Zhanga, J.; Lia, H.; Changa, X.; Zhua, L.; Xuea, Q. Enhanced gas separation performance of Pebax mixed matrix membranes by incorporating ZIF-8 in situ inserted by multiwalled carbon nanotubes. *Sep. Purif. Technol.* **2020**, *248*, 117080. [[CrossRef](#)]
153. Moghadam, F.; Lee, T.H.; Park, I.; Park, H.B. Thermally annealed polyimide-based mixed matrix membrane containing ZIF-67 decorated porous graphene oxide nanosheets with enhanced propylene/propane selectivity. *J. Membr. Sci.* **2020**, *603*, 118019. [[CrossRef](#)]
154. Wong, K.C.; Goh, P.; Taniguchi, T.; Ismail, A.F.; Zahri, K. The role of geometrically different carbon-based fillers on the formation and gas separation performance of nanocomposite membranes. *Carbon* **2019**, *149*, 33–44. [[CrossRef](#)]
155. Shi, F.; Sun, J.; Wang, J.; Liu, M.; Wang, S.; Cao, X.; Yan, Z.; Li, Y.; Nunes, S.P. Exploration of the Synergy Between 2D Nanosheets and a Non-2D Filler in Mixed Matrix Membranes for Gas Separation. *Front. Chem.* **2020**, *8*, 1–12. [[CrossRef](#)]
156. Sivakumar, M.; Liu, D.-K.; Chiao, Y.-H.; Hung, W.-S. Synergistic effect of one-dimensional silk nanofiber and two-dimensional graphene oxide composite membrane for enhanced water purification. *J. Membr. Sci.* **2020**, *606*, 118142. [[CrossRef](#)]
157. Zhu, L.; Wang, H.; Bai, J.; Liu, J.; Zhang, Y. A porous graphene composite membrane intercalated by halloysite nanotubes for efficient dye desalination. *Desalination* **2017**, *420*, 145–157. [[CrossRef](#)]
158. Liu, Y.; Wang, X.; Gao, X.; Zheng, J.; Wang, J.; Volodin, A.; Xie, Y.F.; Huang, X.; Van Der Bruggen, B.; Zhu, J. High-performance thin film nanocomposite membranes enabled by nanomaterials with different dimensions for nanofiltration. *J. Membr. Sci.* **2020**, *596*, 117717. [[CrossRef](#)]
159. Dong, L.; Li, M.; Zhang, S.; Si, X.; Bai, Y.; Zhang, C. NH<sub>2</sub>-Fe<sub>3</sub>O<sub>4</sub>-regulated graphene oxide membranes with well-defined laminar nanochannels for desalination of dye solutions. *Desalination* **2020**, *476*, 114227. [[CrossRef](#)]
160. Wang, J.; Wang, Y.; Zhu, J.; Zhang, Y.; Liu, J.; Van Der Bruggen, B. Construction of TiO<sub>2</sub>@graphene oxide incorporated antifouling nanofiltration membrane with elevated filtration performance. *J. Membr. Sci.* **2017**, *533*, 279–288. [[CrossRef](#)]
161. Zhu, C.; Liu, G.; Han, K.; Ye, H.; Wei, S.; Zhou, Y. One-step facile synthesis of graphene oxide/TiO<sub>2</sub> composite as efficient photocatalytic membrane for water treatment: Crossflow filtration operation and membrane fouling analysis. *Chem. Eng. Process. Process. Intensif.* **2017**, *120*, 20–26. [[CrossRef](#)]

162. Abadikhah, H.; Kalali, E.N.; Khodi, S.; Xu, X.; Agathopoulos, S. Multifunctional Thin-Film Nanofiltration Membrane Incorporated with Reduced Graphene Oxide@TiO<sub>2</sub>@Ag Nanocomposites for High Desalination Performance, Dye Retention, and Antibacterial Properties. *ACS Appl. Mater. Interfaces* **2019**, *11*, 23535–23545. [[CrossRef](#)] [[PubMed](#)]
163. Dadvar, E.; Kalantary, R.R.; Panahi, H.A.; Peyravi, M. Efficiency of Polymeric Membrane Graphene Oxide-TiO<sub>2</sub> for Removal of Azo Dye. *J. Chem.* **2017**, *2017*, 1–13. [[CrossRef](#)]
164. Xu, Y.; Peng, G.; Liao, J.; Shen, J.; Gao, C. Preparation of molecular selective GO/DTiO<sub>2</sub>-PDA-PEI composite nanofiltration membrane for highly pure dye separation. *J. Membr. Sci.* **2020**, *601*, 601. [[CrossRef](#)]
165. Chung, Y.T.; Mahmoudi, E.; Mohammad, A.W.; Benamor, A.; Johnson, D.; Hilal, N. Development of polysulfone-nanohybrid membranes using ZnO-GO composite for enhanced antifouling and antibacterial control. *Desalination* **2017**, *402*, 123–132. [[CrossRef](#)]
166. Chen, L.; Li, N.; Wen, Z.; Zhang, L.; Chen, Q.; Chen, L.; Si, P.; Feng, J.; Li, Y.; Lou, J.; et al. Graphene oxide based membrane intercalated by nanoparticles for high performance nanofiltration application. *Chem. Eng. J.* **2018**, *347*, 12–18. [[CrossRef](#)]
167. Liu, G.-F.; Huang, L.-J.; Wang, Y.-X.; Tang, J.; Wang, Y.; Cheng, M.-M.; Zhang, Y.; Kipper, M.J.; Belfiore, L.A.; Ranil, W.S. Preparation of a graphene/silver hybrid membrane as a new nanofiltration membrane. *RSC Adv.* **2017**, *7*, 49159–49165. [[CrossRef](#)]
168. Ma, Z.; Liang, S.; Zhang, S.; Xiao, K.; Wang, X.; Li, M.; Huang, X. Surface functionalization via synergistic grafting of surface-modified silica nanoparticles and layered double hydroxide nanosheets for fabrication of superhydrophilic but relatively oleophobic antifouling membranes. *Sep. Purif. Technol.* **2020**, *247*, 116955. [[CrossRef](#)]
169. Modi, A.; Bellare, J.R. Efficient separation of biological macromolecular proteins by polyethersulfone hollow fiber ultrafiltration membranes modified with Fe<sub>3</sub>O<sub>4</sub> nanoparticles-decorated carboxylated graphene oxide nanosheets. *Int. J. Biol. Macromol.* **2019**, *135*, 798–807. [[CrossRef](#)]
170. Lee, T.H.; Roh, J.S.; Yoo, S.Y.; Roh, J.M.; Choi, T.H.; Park, H.B. High-Performance Polyamide Thin-Film Nanocomposite Membranes Containing ZIF-8/CNT Hybrid Nanofillers for Reverse Osmosis Desalination. *Ind. Eng. Chem. Res.* **2020**, *59*, 5324–5332. [[CrossRef](#)]
171. Zeng, G.; He, Y.; Ye, Z.; Yang, X.; Chen, X.; Ma, J.; Li, F. Novel Halloysite Nanotubes Intercalated Graphene Oxide Based Composite Membranes for Multifunctional Applications: Oil/Water Separation and Dyes Removal. *Ind. Eng. Chem. Res.* **2017**, *56*, 10472–10481. [[CrossRef](#)]
172. Han, Y.; Jiang, Y.; Gao, C. High-Flux Graphene Oxide Nanofiltration Membrane Intercalated by Carbon Nanotubes. *ACS Appl. Mater. Interfaces* **2015**, *7*, 8147–8155. [[CrossRef](#)]
173. Gao, S.J.; Qin, H.; Liu, P.; Jin, J. SWCNT-intercalated GO ultrathin films for ultrafast separation of molecules. *J. Mater. Chem. A* **2015**, *3*, 6649–6654. [[CrossRef](#)]
174. Zengab, H.; YuABC, Z.; Shaoab, L.; Liab, X.; Zhuab, M.; Liuab, Y.; Fengab, X.; Zhuab, X. Ag<sub>2</sub>CO<sub>3</sub>@UiO-66-NH<sub>2</sub> embedding graphene oxide sheets photocatalytic membrane for enhancing the removal performance of Cr(VI) and dyes based on filtration. *Desalination* **2020**, *491*, 114558. [[CrossRef](#)]
175. Chen, L.; Wang, W.; Fang, Q.; Zuo, K.; Hou, G.; Ai, Q.; Li, Q.; Ci, L.; Lou, J. High performance hierarchically nanostructured graphene oxide/covalent organic framework hybrid membranes for stable organic solvent nanofiltration. *Appl. Mater. Today* **2020**, *20*, 100791. [[CrossRef](#)]
176. Xie, A.; Cui, J.; Yang, J.; Chen, Y.; Lang, J.; Li, C.; Yan, Y.; Dai, J. Graphene oxide/Fe(III)-based metal-organic framework membrane for enhanced water purification based on synergistic separation and photo-Fenton processes. *Appl. Catal. B Environ.* **2020**, *264*, 118548. [[CrossRef](#)]
177. Khan, N.A.; Yuan, J.; Wu, H.; Cao, L.; Zhang, R.; Liu, Y.-N.; Li, L.; Rahman, A.U.; Kasher, R.; Jiang, Z. Mixed Nanosheet Membranes Assembled from Chemically Grafted Graphene Oxide and Covalent Organic Frameworks for Ultra-high Water Flux. *ACS Appl. Mater. Interfaces* **2019**, *11*, 28978–28986. [[CrossRef](#)]
178. Song, N.; Sun, Y.; Xie, X.; Wang, D.; Shao, F.; Yu, L.; Dong, J. Doping MIL-101(Cr)@GO in polyamide nanocomposite membranes with improved water flux. *Desalination* **2020**, *492*, 114601. [[CrossRef](#)]
179. Zeng, H.; Yu, Z.; Shao, L.; Li, X.; Zhu, M.; Liu, Y.; Feng, X.; Zhu, X. A novel strategy for enhancing the performance of membranes for dyes separation: Embedding PAA@UiO-66-NH<sub>2</sub> between graphene oxide sheets. *Chem. Eng. J.* **2021**, *403*, 126281. [[CrossRef](#)]

180. Guan, K.; Zhao, D.; Zhang, M.; Shen, J.; Zhou, G.; Liu, G.; Jin, W. 3D nanoporous crystals enabled 2D channels in graphene membrane with enhanced water purification performance. *J. Membr. Sci.* **2017**, *542*, 41–51. [[CrossRef](#)]
181. Su, B.; Wu, Y.; Jiang, L. The art of aligning one-dimensional (1D) nanostructures. *Chem. Soc. Rev.* **2012**, *41*, 7832–7856. [[CrossRef](#)] [[PubMed](#)]
182. Goh, P.; Ismail, A.; Ng, B. Directional alignment of carbon nanotubes in polymer matrices: Contemporary approaches and future advances. *Compos. Part A Appl. Sci. Manuf.* **2014**, *56*, 103–126. [[CrossRef](#)]
183. Karunakaran, M.; Shevate, R.; Kumar, M.; Peinemann, K.V. CO<sub>2</sub>-selective PEO-PBT (PolyActive™)/graphene oxide composite membranes. *Chem. Commun.* **2015**, *51*, 14187–14190. [[CrossRef](#)] [[PubMed](#)]
184. Zhang, Y.; Shen, Q.; Hou, J.; Sutrisna, P.D.; Chen, V. Shear-aligned graphene oxide laminate/Pebax ultrathin composite hollow fiber membranes using a facile dip-coating approach. *J. Mater. Chem. A* **2017**, *5*, 7732–7737. [[CrossRef](#)]
185. Liu, C.; Wang, W.; Zhu, L.; Cui, F.; Xie, C.; Chen, X.; Li, N. High-performance nanofiltration membrane with structurally controlled PES substrate containing electrically aligned CNTs. *J. Membr. Sci.* **2020**, *605*, 118104. [[CrossRef](#)]
186. Qin, L.; Zhao, Y.; Liu, J.-D.; Hou, J.; Zhang, Y.; Wang, J.; Zhu, J.; Zhang, B.; Lvov, Y.; Van Der Bruggen, B. Oriented Clay Nanotube Membrane Assembled on Microporous Polymeric Substrates. *ACS Appl. Mater. Interfaces* **2016**, *8*, 34914–34923. [[CrossRef](#)]
187. Hinds, B.J.; Chopra, N.; Rantell, T.; Andrews, R.; Gavalas, V.; Bachas, L.G. Aligned Multiwalled Carbon Nanotube Membranes. *Science* **2004**, *303*, 62–65. [[CrossRef](#)]
188. Samieirad, S.; Mousavi, S.M.; Saljoughi, E. Alignment of functionalized multiwalled carbon nanotubes in forward osmosis membrane support layer induced by electric and magnetic fields. *Powder Technol.* **2020**, *364*, 538–552. [[CrossRef](#)]
189. Li, M.; Brant, J.A. Effects of aluminogermanate imogolite nanotube orientation on mass transport across polyamide nanocomposite membranes. *J. Membr. Sci.* **2019**, *585*, 38–51. [[CrossRef](#)]
190. Xie, K.; Fu, Q.; Qiao, G.G.; Webley, P.A. Recent progress on fabrication methods of polymeric thin film gas separation membranes for CO<sub>2</sub> capture. *J. Membr. Sci.* **2019**, *572*, 38–60. [[CrossRef](#)]
191. Yunker, P.J.; Still, T.; Lohr, M.A.; Yodh, A.G. Suppression of the coffee-ring effect by shape-dependent capillary interactions. *Nat. Cell Biol.* **2011**, *476*, 308–311. [[CrossRef](#)] [[PubMed](#)]
192. Guan, L.-Z.; Zhao, L.; Wan, Y.-J.; Tang, L.-C. Three-dimensional graphene-based polymer nanocomposites: Preparation, properties and applications. *Nanoscale* **2018**, *10*, 14788–14811. [[CrossRef](#)] [[PubMed](#)]
193. Nishihara, H.; Kyotani, T. Zeolite-templated carbons—three-dimensional microporous graphene frameworks. *Chem. Commun.* **2018**, *54*, 5648–5673. [[CrossRef](#)] [[PubMed](#)]
194. Sui, X.; Ding, H.; Yuan, Z.; Leong, C.F.; Goh, K.; Li, W.; Yang, N.; D’Alessandro, D.M.; Chen, Y. The roles of metal-organic frameworks in modulating water permeability of graphene oxide-based carbon membranes. *Carbon* **2019**, *148*, 277–289. [[CrossRef](#)]

**Publisher’s Note:** MDPI stays neutral with regard to jurisdictional claims in published maps and institutional affiliations.



© 2020 by the authors. Licensee MDPI, Basel, Switzerland. This article is an open access article distributed under the terms and conditions of the Creative Commons Attribution (CC BY) license (<http://creativecommons.org/licenses/by/4.0/>).